NE

LLL: UCRL-52533
NASA: CR-159512

HIGH-PERFORMANCE FIBER/ EPOXY COMPOSITE PRESSURE VESSELS

T. T. Chiao, M. A. Hamstad, E. S. Jessop, and R. H. Toland

December 12, 1978

Work performed under the auspices of the U.S. Department of Energy by the UCLLL under contract number W-7405-ENG-48.

Printed in the United States of America
Available from
National Technical Information Service
U.S. Department of Commerce
5285 Port Royal Road
Springfield, VA 22161
Price: Printed Copy $; Microfiche $3.00

Page Range	Domestic Price	Page Range	Domestic Price
001 025	$ 4.00	326 350	$12.00
026 050	4.50	351 375	12.50
051 075	5.25	376 400	13.00
076 100	6.00	401 425	13.25
101 125	6.50	426 450	14.00
126 150	7.25	451 475	14.50
151 175	8.00	476 500	15.00
176 200	9.00	501 525	15.25
201 225	9.25	526 550	15.50
226 250	9.50	551 575	16.25
251 275	10.75	576 600	16.50
276 300	11.00	601 up	[1]
301 325	11.75		

[1] Add $2.50 for each additional 100 page increment from 601 pages up.

Distribution Category
UC-94b

LAWRENCE LIVERMORE LABORATORY
University of California Livermore, California 94550

LLL: UCRL-52533
NASA: CR-159512

HIGH-PERFORMANCE FIBER/ EPOXY COMPOSITE PRESSURE VESSELS

T. T. Chiao, M. A. Hamstad, E. S. Jessop, and R. H. Toland*

MS. Date: December 12, 1978

*R. H. Toland's current address is United Engineers, 30 South 17th Street, Philadelphia, PA 19101.

PREFACE

This is an interim report of the LLL effort on NASA Contract No. C-13980-C, NASA-Lewis Research Center, R. F. Lark, Project Manager, covering the period from 1974 through 1976. The objective of this effort is to develop high-performance, lightweight, filament wound, composite pressure vessels. This technology is valuable to the NASA Space Shuttle Programs and to many potential commercial ventures.

CONTENTS

HIGH-PERFOR NCE FIBER/ EPOXY COMPOSITE PRESSURE VESSELS

ABSTRACT

During the 1974-1976 report period our principal efforts were directed in the following areas:

- Determining the applicability of an ultrahigh-strength graphite fiber to composite pressure vessels.
- Defining the fatigue performance of thin-titanium-lined, high-strength graphite/epoxy pressure vessels.
- Selecting epoxy resin systems suitable for filament winding.
- Studying the fatigue life potential of Kevlar 49/epoxy pressure vessels.
- Developing polymer liners for composite pressure vessels.

The fiber performance and potential as a reinforcement for composites of the Thornel Special graphite fiber were evaluated by testing fiber/epoxy strands. Properties determined were fiber uniformity, strength and modulus at room and liquid nitrogen temperatures, stress-strain behavior, effect of strain rate on fiber strength, and acoustic emission during tensile loading to failure. The Thornel Special graphite fiber was found to have a 3570-MPa failure stress, a 1.7% failure strain, a 206-GPa modulus, and a 1.77-Mg/m^3 density at 23°C. Low temperature and various strain rates appear to have no significant effect on fiber tensile properties.

We then used this graphite fiber in a program to develop thin-metal-lined fiber/epoxy pressure vessels with fatigue lives greater than 1000 load cycles. The performance factor of the composite (burst pressure × vessel volume ÷ composite mass) was found to be 351 kPa·m^3/kg. Both aluminum-lined and titanium-lined pressure vessels were then filament wound with the graphite fiber in an epoxy matrix. By subjecting vessels to hydraulic cyclic fatigue testing to about 50% of the expected burst pressure, the average fatigue lives of the aluminum-lined and titanium-lined vessels were determined to be 462 and 2190 cycles, respectively.

We also conducted a study to formulate and select a state-of-the-art epoxy resin for wet filament winding. Pressure vessels using the high-modulus, high-strength Kevlar 49 fiber were wound with ten different epoxy systems. We determined fiber strand strength, shear strength, and vessel performance for the different epoxies. On the basis of processibility, neat resin properties, and vessel performance, an epoxy system based on the rubber-modified bisphenol F resin, diluted with vinylcyclohexane dioxide, and cured with mixed aromatic amines was found to yield overall performance comparable to the epoxy system based on the bisphenol A resin, diluted with bis(2,3-epoxycyclopentyl)ether.

Next, we attempted to develop fatigue-resistant polymer liners for pressure vessels to contain nitrogen gas at room temperature. The nitrogen permeability of chlorobutyl rubber sheet, coated with Saran, Parylene C, or both, was determined in flat specimens. Four 10-cm-diameter, cylindrical Kevlar 49/epoxy pressure vessels were fabricated with chlorobutyl rubber liners coated with the polymers. These vessels were pressurized with nitrogen gas and then valved off to about 65% (11.7 MPa) of the expected failure pressure. One vessel leaked; the other three showed an average pressure loss of less than 1% per month.

The cyclic fatigue life of Kevlar/epoxy pressure vessels also was determined. Twenty-five vessels were pressurized internally until they burst. Twenty-five vessels were tested under sinusoidal cycling at 1 Hz, between 4% and 91% of the mean burst pressure. Twenty-five more

vessels were tested between 4% and 91% of mean burst strength with a rectangular pressure pulse at 0.33 Hz. A few vessels also were tested for stress-rupture at the 91% load level. Cyclic fatigue was found to depend on the time spent at peak load and on the number of stress cycles.

We fabricated Kevlar 49/epoxy and graphite fiber/epoxy pressure vessels, 10.2 cm in diameter, some with aluminum liners and some with alternating layers of rubber and polymer. To determine liner performance, we subjected vessels to gas permeation tests, fatigue cycling, and burst tests, measuring composite performance, fatigue life, and leak rates. Both the metal and the rubber/polymer liner performed well. Next, we fabricated proportionately larger pressure vessels (20.3 and 38 cm in diameter) and subjected them to the same tests. In these larger vessels, we encountered liner leakage problems with both liners; the causes of the leaks were identified and some solutions to such liner problems are recommended. However, we have yet to produce a successful, large-scale, polymer-lined pressure vessel.

PART I. ULTRAHIGH-STRENGTH GRAPHITE FIBER FOR PRESSURE VESSEL APPLICATIONS

Properties of Graphite Fiber

We have examined the performance of an ultrahigh-strength, low-density graphite fiber that is being considered for filament wound pressure vessels designed for possible space shuttle applications. A polyacrylonitrile (PAN) based graphite fiber (Thornel Special) is available by special order; the properties claimed by the manufacturer, Union Carbide Corporation, appeared very attractive for tensile-critical applications. Therefore, we thoroughly characterized this fiber in fiber/epoxy composites from an engineering point of view. We determined fiber uniformity, various tensile properties, stress-rupture behavior, fiber processibility in the filament winding process, and performance of the fiber in pressure vessels.

Fiber Characterization

The Thornel Special graphite fiber is made from a single-end, 1500-filament PAN precursor. The elemental analysis is carbon 88.59%, hydrogen 0.30%, nitrogen 7.609%, chlorine 3.00%, ash 0.04%, and oxygen 0.47% (by difference). The fiber strand is slightly twisted, approximately 0.15 turns/cm. Average fiber density, determined from three tests where the fiber was immersed in kerosene and compared against a calibrated quartz standard, is 1.77 Mg/m^3 at 23 C. In many ways, this graphite fiber is similar to the commercially available Thornel 400 graphite fiber, also from the Union Carbide Corporation.

Thirty spools of graphite fiber were selected from several batches. We took three 2.54-m-long specimens from each spool and checked the weight variation of the fiber strands. Figure 1 is a summary of these data in denier (g/9000 m). The equivalent cross-sectional area of the fiber strands was calculated using the fiber density and the average fiber mass of the three specimens from each spool. The results are shown in Fig. 2. The 3.5% coefficient of variation (CV) is considered small. The average cross-sectional area of 4.022×10^{-4} cm^2 can be used for converting tensile load to fiber stress in most engineering calculations.

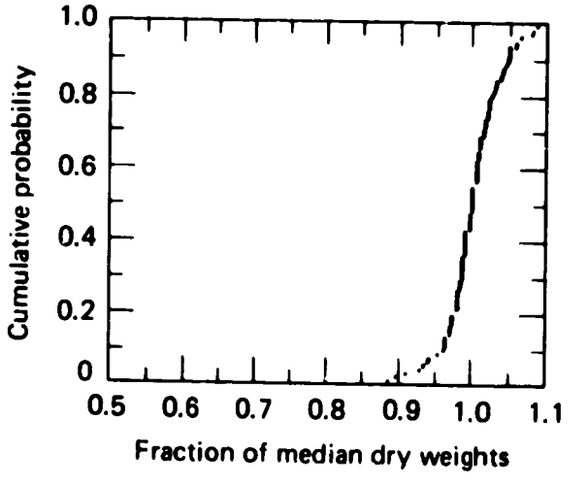

Fig. 1. Denier variation of the Thornel Special graphite fiber: average 641, median 640, standard deviation 24, CV 3.7%, N 90.

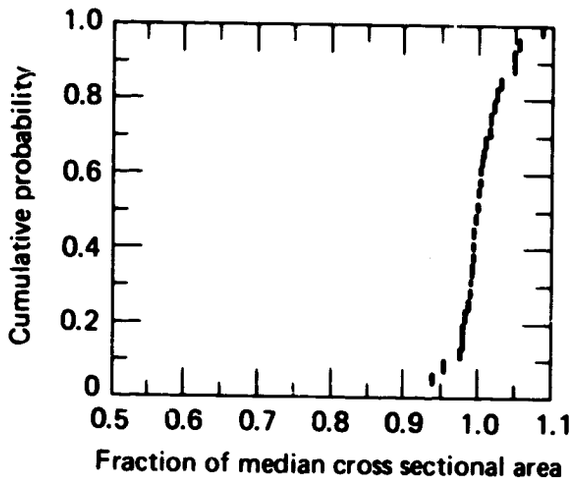

Fig. 2. Cross-sectional area of the Thornel Special graphite fiber: average = 4.022 × 10⁻⁴ cm², medium = 4.014 × 10⁻⁴ cm², standard deviation = 0.142 × 10⁻⁴ cm², CV = 3.5%, N = 30.

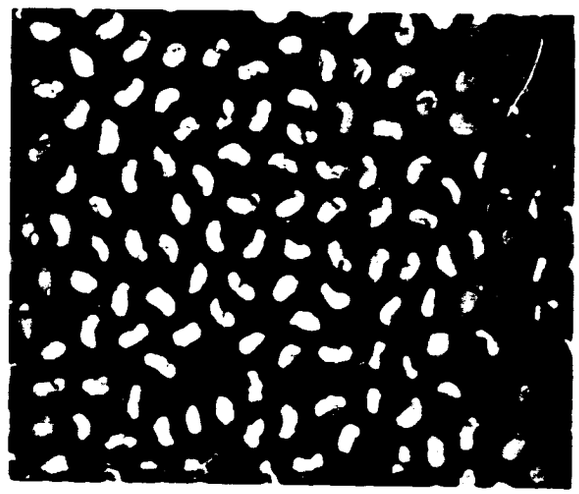

Fig. 3. Photograph of fiber filament shapes.

The Matrix System

We used a room-temperature-curable epoxy system, DER 332[1]/Jeffamine T-403[2] (100/36 parts by weight), throughout the study. The pure resin system, when gelled at ambient temperature overnight and cured at 74°C for 3 h, has a typical tensile rupture strength of 75.2 MPa, a rupture elongation of 5%, and a modulus of 3.4 GPa. We have previously studied this resin system in detail.[2]

Fiber/Epoxy Strands

We used epoxy-impregnated fiber strand specimens to determine the tensile properties of the graphite fiber. Over 5000 composite strands (approximately 180 fiber strands from each spool) were fabricated using a vacuum filament winding process. From a random spool of fiber, we made almost 2000 more composite specimens to study the effect of strain rate and liquid nitrogen temperature on fiber tensile strength. Similar strand specimens also are being used to check the stress-rupture behavior of the fiber composite. The strands were impregnated with the epoxy system described above and cured following the same schedule. We determined the fiber volume content of 10 fiber/epoxy strands selected randomly from each group of 180 specimens. The fiber content of these strands averaged 64.2 vol%, with a CV of 8.7%. The fiber filament shapes are shown in Fig. 3.

Using a 25.4-cm gage length, we tested the tensile strength of the strands at a constant crosshead speed of 1 cm/min with a simple clamping arrangement. Our machine compliance was measured by varying the gage length of the specimens. We used over 500 strand specimens to study the stress-strain behavior of the Thornel Special graphite fiber. Figure 4 shows a typical stress-strain curve: the ordinate indicates only the fiber stress,[3] not the composite stress. The distribution of the fiber failure properties as well as the fiber modulus are summarized in Fig. 5. The average fiber properties—a failure stress of 3570 MPa, a failure strain of 1.7%, and a modulus of 206 GPa—are truly outstanding among graphite fibers. However, the data scatter, as indicated by a CV greater than 9%, is undesirably high.

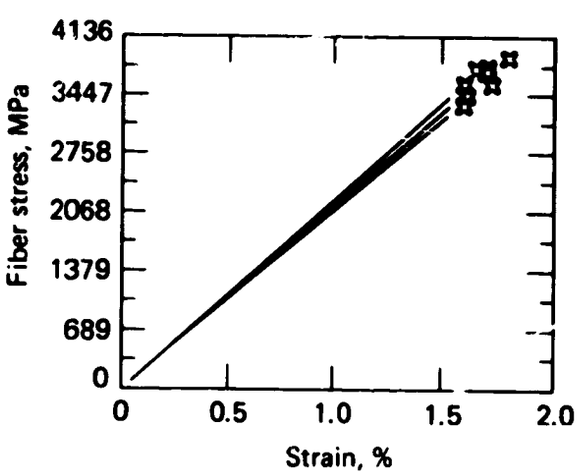

Fig. 4. Typical stress-strain curve of the Thornel Special graphite fiber calculated from epoxy-impregnated strands.

[1] Dow Chemical Company
[2] Jefferson Chemical Company

[3] Fiber stress was calculated by ignoring the matrix contribution in the strands

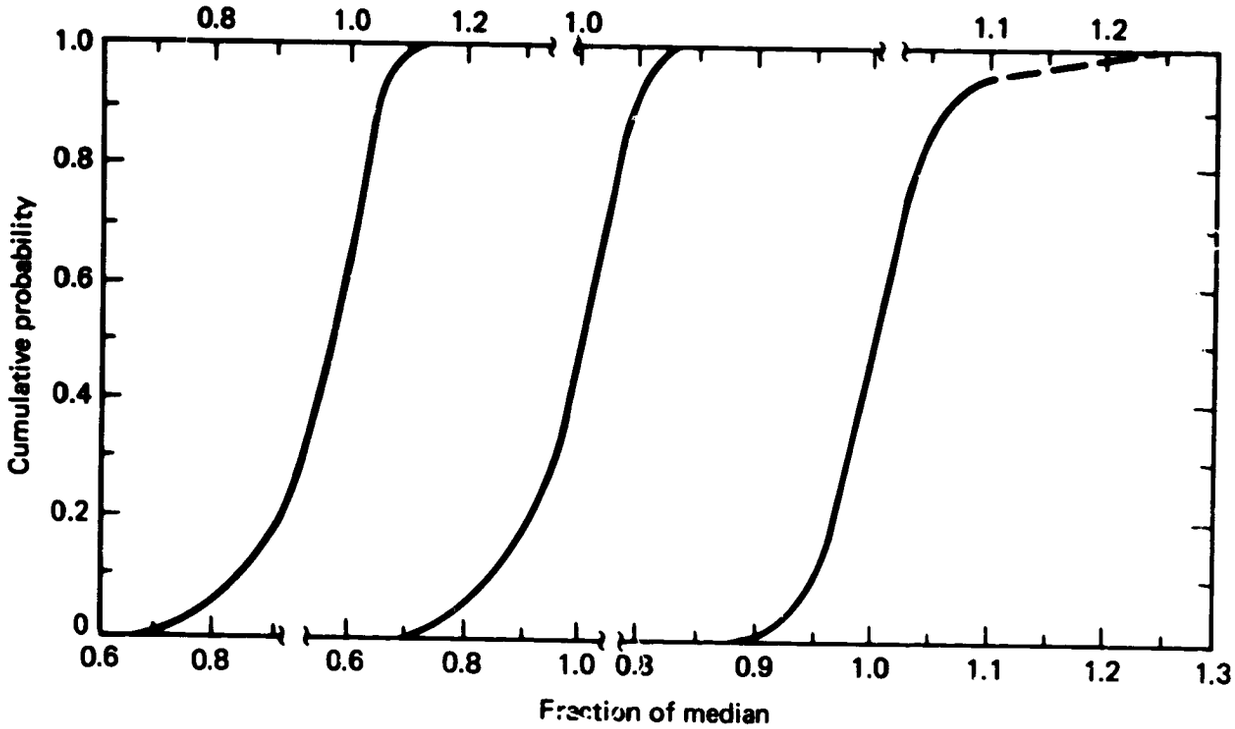

Rupture stress	Rupture strain	Modulus
Average = 3570 MPa	Average = 1.7	Average = 206 GPa
Median = 3640 MPa	Median = 1.7	Median = 205 GPa
Std dev = 330 MPa	Std dev = 0.2	Std dev = 11 GPa
CV = 9.3%	CV = 9.6%	CV = 5.3%
N = 557	N = 556	N = 557

Fig. 5. Tensile properties of the Thornel Special graphite fiber/epoxy strands.

The effect of low temperature on fiber strength was determined by immersing composite strand specimens directly into liquid nitrogen. We used a 12.7-cm gage length in this study. On the basis of tests performed at room temperature and liquid nitrogen temperature (Table 1), it is apparent that temperature over this range does not affect the fiber tensile properties.

The effect of strain rate on the fiber tensile properties is of interest to many researchers. Table 2 shows such data based on strand specimens from the spool of fiber used for the previous tests. The strain rate effect, if any, is minimal. We note that the minimal effects of strain rate and liquid nitrogen temperature are consistent with our previous data on many advanced fibers.[3-5]

Table 1. Tensile properties of Thornel Special graphite fiber/epoxy strands at room and liquid nitrogen temperatures: 50 and [illegible] specimens, all made from a single spool of fiber, were tested at room and liquid nitrogen temperatures, respectively.

Property	Room temperature, 21°C	Liquid nitrogen temperature, −196°C
Average tensile rupture stress of fiber,* MPa (CV, %)	3839 (4.0)	3659 (7.5)
Fiber modulus at 0.5% strain, GPa (CV, %)	205 (3.1)	201 (5.4)
Rupture strain, % (CV, %)	1.8 (5.2)	1.9 (9.6)

*Fiber stress was calculated by ignoring the matrix contribution in the strand specimens.

Table 2. Strain rate effect on the tensile properties of Thornel Special graphite fiber/epoxy strands (10 specimens tested at each strain rate).

Property	Strain rate, min^{-1}				
	1.97	1.95×10^{-1}	1.97×10^{-2}	1.97×10^{-3}	1.97×10^{-4}
Rupture stress, MPa (CV, %)	3860 (5.6)	3880 (4.0)	3780 (7.4)	3650 (4.1)	3690 (2.5)
Secant modulus at 0.5% strain, GPa (CV, %)	—	—	209 (1.1)	208 (2.2)	208 (2.8)
Rupture strain, % (CV, %)	—	—	1.7 (8.2)	1.7 (5.1)	1.7 (3.5)

In searching for a nondestructive test to study the failure of fiber composites, we found that acoustic emission (AE) monitoring is most promising. We tested 30 graphite fiber/epoxy strands under tensile loading using AE monitoring. A typical plot of AE vs fiber stress is shown in Fig. 6. The signal counts are associated mainly with fiber failures. As indicated in Fig. 6, no fiber damage was detected until the applied load exceeded 1380 MPa, approximately one-third the ultimate fiber failure stress.

We also studied the long-term performance (stress-rupture) of the Thornel Special graphite fiber/epoxy strands. We took another 100 specimens made from the spool of fiber used previously and loaded them to 90% of the average fiber failure stress. The limited data show that this graphite fiber/epoxy composite is superior to other composite systems, such as aramid fiber/epoxy and S-glass/epoxy.

Applications of Graphite Fiber to Pressure Vessels

Basis for Study

The development of high-strength fibers and the filament-winding process has made possible the manufacture of high-performance filament wound composite pressure vessels. These vessels often have a composite performance factor (i.e., failure pressure × volume ÷ mass) at least double that of titanium vessels. Because pressurizing a composite vessel causes the matrix to crack, unlined composite vessels are permeable even to liquids. To overcome this problem, the usual manufacturing technique is to filament-wind the fiber/epoxy composite over a metal liner. The liner acts as a bladder and prevents leakage of the fluid stored in the pressure vessel; the filament overwrap provides the necessary strength. This technique has been most successful for applications where fatigue loading is not severe.

A lightweight filament wound pressure vessel is appealing to the NASA Space Shuttle program. One application requires the containment of gases at room temperature plus a minimum vessel fatigue life greater than 1000 cycles. To date, lightweight, thin metal lined composite pressure vessels have not met the lifetime requirement for two basic reasons. First, during each pressure cycle, the metal liner yields and experiences significant plastic deformation both on pressurization and on depressurization. Significant plastic deformation leads to poor fatigue life in metals. Thus, after relatively few cycles, cracks develop in the metal liner and the pressure vessel leaks. These cracks occur most often in the liner welds or weld regions because the weld strength is usually less than that of the parent metal. Second, for very thin liners, failure of the adhesive bond between the metal liner and the composite allows the liner to buckle on depressurization. Because of this repeated buckling, the liner cracks usually after only a few more cycles.

To overcome these fatigue life problems, we incorporated several new concepts into our pressure

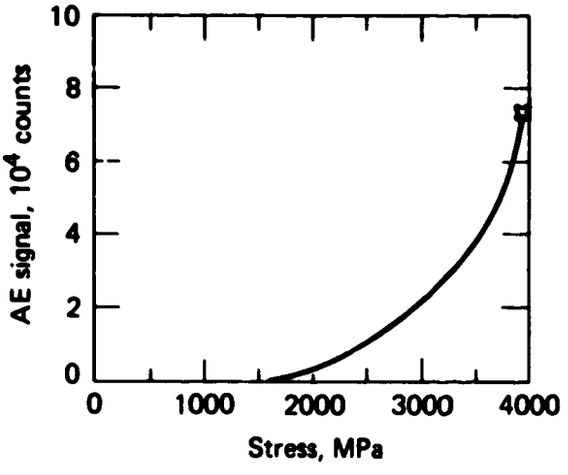

Fig. 6. Typical curve of fiber stress vs AE signal counts under tensile loading of the Thornel Special graphite fiber/epoxy strands: gain = 80 dB, bandwidth = 100 to 300 kHz.

vessels. First, we used the experimental, fairly high-modulus, ultrahigh-strength Thornel Special graphite fiber. Although a high-modulus fiber would greatly alleviate the metal liner problem, the commercially available high-modulus fibers lack the strength of the glass or aramid fibers. Our choice of the Thornel Special graphite fiber was the best available compromise. Second, we used a metal liner with a high yield strength, hypothesizing that the plastic deformation of a high-yield-strength liner would not be as severe as with a lower-yield-strength metal. Third, we used a moderately thin liner rather than an ultrathin liner so that the buckling resistance of the liner would not depend so heavily on maintaining the integrity of the liner-to-composite bond. The increased liner thickness also would help provide better dimensional control of the liner during machining and welding. Fourth, we made as few welds as possible and used metal liner materials with weld-region yield strength as close as possible to the yield strength of the parent metal.

Winding Study of Graphite Fiber/Epoxy Pressure Vessels[6]

We fabricated a number of 10.2-cm-diameter, chlorobutyl-rubber-lined pressure vessels to determine the composite and fiber performance of our vessel design (see Fig. 7). After testing some preliminary vessel designs, we defined our winding pattern and wound 18 vessels on a numerically controlled winding machine. The epoxy system used was XD 7818 (Dow Chemical Co.) with Jeffamine T-403. During winding, the fiber/epoxy impregnation operation was conducted inside a vacuum chamber held at approximately 658 Pa; we used a constant 4.5-N winding tension.

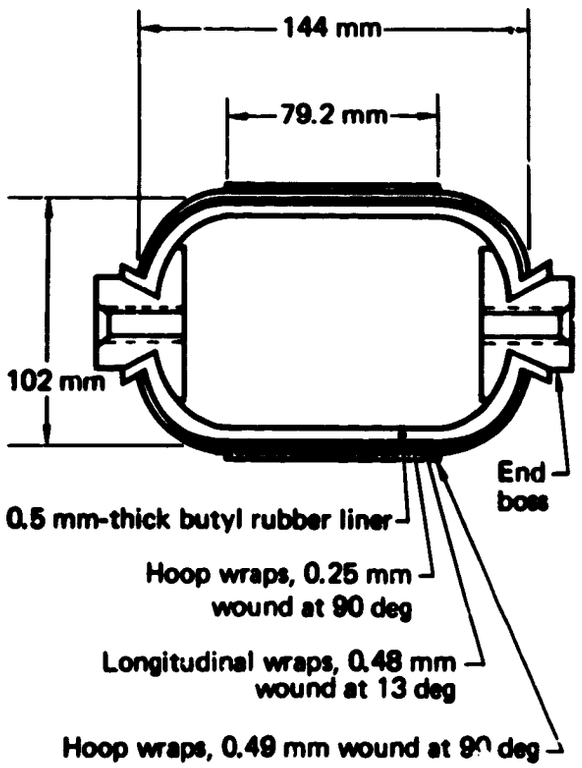

Fig. 7. Typical dimensions of a 10.2-cm-diameter, filament wound pressure vessel (volume = 950 ± 8 cm³).

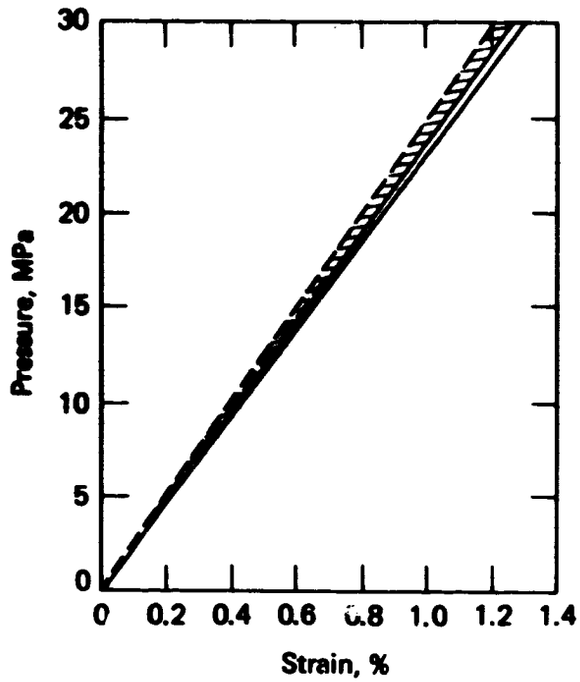

Fig. 8. Pressure vs deformation curves from three rubber-lined, 10.2-cm-diameter, Thornel Special graphite fiber/epoxy vessels: solid lines denote the hoop strain band, dashed lines denote the axial strain band.

The details of the winding pattern, cure, and vessel performance are given in Table 3. The vessels were hydraulically burst with oil at a constant pressurization rate of 6.9 MPa/min using a feedback control system. Figure 8 shows the pressure vs deformation curves for three of these vessels. The strains were obtained from strain gages attached to the outer hoop layer of the pressure vessels.

From these results, several points are apparent. First, the average vessel performances are significantly higher than we previously found for another graphite fiber/epoxy composite,[7] where we reported a graphite/epoxy vessel performance of 0.286 MPa·m³/kg. In the present study, the average vessel performance factor was found to be 0.450 MPa·m³/kg. This performance factor is better than that found for S-glass but less than that determined for Kevlar 49. Second, the data scatter in terms of vessel burst pressure or vessel performance factor is still rather

Table 3. Specifications for and performance of 18 rubber-lined, Thornel Special graphite fiber/epoxy[a] pressure vessels (CS-18 through CS-35): rubber liner thickness = 0.5 mm, test temperature = 23°C.

Data	18-vessel average	CV, %	Maximum value	Minimum value
Vessel Data				
Volume, V, 10^{-4} m³	9.483			
Burst pressure, P, MPa	25.72	7.6	30.54	23.06
Failure location	mixed			
Performance factor, MPa·m³/kg: fiber, PV/W_f	0.451	7.4	0.535	0.399
composite, PV/W_c	0.351	7.5	0.411	0.316
Composite Data				
Mass, kg: fiber, W_f	0.0542	3.6		
composite, W_c	0.0699	4.0		
Fiber content, vol%	62.8	2.8		
Vessel wall thickness, mm: hoop	0.74			
longitudinal	0.48			
Winding Data				
Longitudinal angle, deg	13			
Hoop-to-longitudinal fiber ratio	1.75			
Winding pattern	36-band, closed			
Layers (interspersing): hoop	6 (2 + 4)			
longitudinal	4 (none)			
Total winding circuits: hoop	947			
longitudinal	1080			
Extra reinforcement	none			

[a]Epoxy resin system: XD 7818/T-403 (100/49 parts by weight), gelled for 16 h at 21°C and cured for 3 h at 90°C.

large (e.g., the high burst pressure was 30.5 MPa and the low was 23.0 MPa). The CV, however, was 8.6%, which is less than the CV for the graphite fiber/epoxy strands (9.3%).

Metal-Lined Graphite Fiber/Epoxy Vessels

We next made metal-lined fiber/epoxy pressure vessels 10.2 cm in diameter. The 0.051-cm-thick liners were machined from annealed bar stock with integral fittings. For comparative purposes, liners were made from 5086 aluminum and from 6Al-4V titanium. Figure 9 shows the liner design. The liner halves were electron-beam butt welded with very close tolerances on weld parameters (e.g., drop through, channeling, root porosity). During electron-beam welding, aluminum or titanium rings were bonded in place and were not removed during testing.

Six liners were made from each metal. Before winding, all 12 liners were glass-bead blasted, vapor degreased with trichloroethylene, and then coated with 2 to 4 g of adhesive. The room-temperature-curable epoxy adhesive was Dow XD 7575.02/Dow DER 732/amino-ethylethanolamine (80/20/11.9). The vessels were then filament wound over the metal liners using the same techniques and epoxy as were used for the rubber liners. Essentially the same winding pattern was used for both the metal and rubber liners, except for a slight modification in the number of hoop windings. This modification was made in an attempt to compensate for the partial load-bearing character of the

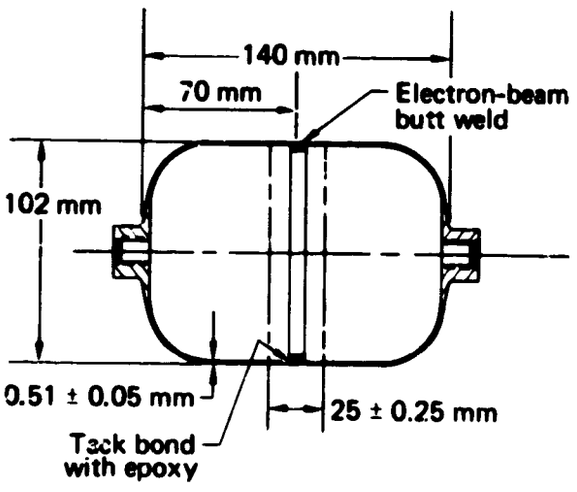

Fig. 9. Design of the metal mandrel used to wind the 10.2-cm-diameter pressure vessels.

metal liners. One vessel of each type was wound and tested. After this, a further modification was made in the winding pattern for the remainder of the vessels. Tables 4 and 5 give the details of the winding patterns and vessel weights of these aluminum- and titanium-lined pressure vessels.

One titanium-lined and one aluminum-lined vessel were burst tested (following the same technique as used for the rubber-lined vessels) to establish the approximate average burst pressure. The performance factor based on total vessel mass, was 0.155 MPa·m³/kg for the titanium-lined vessels and 0.115 MPa·m³/kg for the aluminum-lined vessels. Figure 10 shows typical pressure vs strain curves obtained during these burst tests. The strain gages again were bonded to the outer hoop wraps. The remaining vessels were then proof tested to 50% of the expected burst pressure. Typical strain vs pressure curves of these proof tests are shown in Fig. 11.

After the proof tests, the vessels were hydraulically cycled at 0.33 Hz with a sinusoidal pressure w[illegible]l failure occurred. The peak cyclic pressure v[illegible] of the expected vessel burst pressure. During cyc[illegible], the minimum pressure was 4% (aluminum-lined vessels) and 3% (titanium-lined vessels) of the peak pressures. Tables 6 and 7 summarize the burst pressures, test levels, cyclic lives, and failures for each test. The aluminum-lined vessels (Table 6) had an average cyclic life of 462 cycles (low of 55 cycles and high

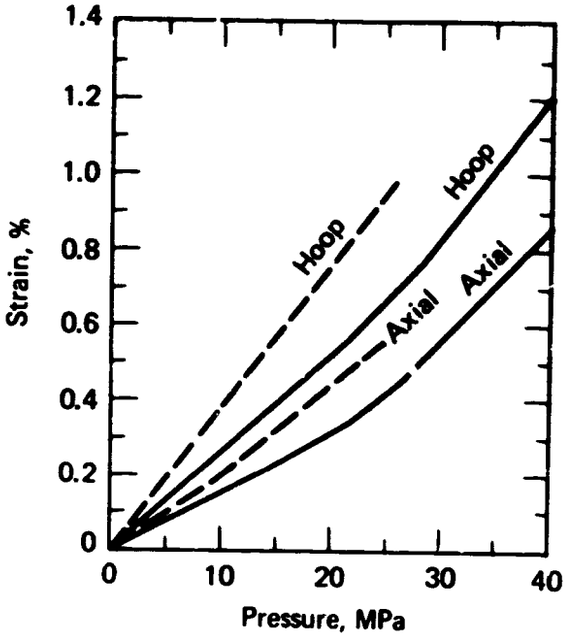

Fig. 10. Pressure vs strain curves for typical titanium-lined and aluminum-lined Thornel Special graphite fiber/epoxy pressure vessels, 10.2 cm in diameter: solid curves denote titanium-lined vessel results, dashed curves denote aluminum-lined vessel results, and the x points denote vessel failures.

Table 4. Winding pattern and fabrication data for Thornel Special graphite fiber/epoxy[a] vessels lined with 0.5-mm-thick aluminum 5086 (vessel volume a constant 0.965 × 10⁻³ m³).

Data	All vessels	Vessel No.					
		CS-36	CS-37	CS-38	CS-39	CS-40	CS-47
Composite Data							
Wall thickness, mm: hoop	0.43						
longitudinal	0.74						
Mass, kg: total vessel[b]		0.1783	0.1769	0.1774	0.1781	0.1770	0.1655
composite		0.0698	0.0666	0.0690	0.0619	0.0689	0.0702
fiber		0.0567	0.0519	0.0541	0.0555	0.0554	0.0600
one boss	0.0125						
adhesive coating	0.002 to 0.004						
Fiber content, vol%		74.4	70.3	70.9	80.2	73.4	80.0
Winding Data							
Longitudinal angle, deg	13						
Winding pattern	36-band, closed						
Hoop-to-longitudinal fiber ratio		1.84	1.75	1.75	1.75	1.75	1.75
Layers (interspersing): hoop	6 (2 + 4)						
longitudinal	4 (none)						
Total winding circuits: hoop		995	947	947	947	947	947
longitudinal	1080						
Extra reinforcement	None						

[a]Epoxy resin system: XD 7818/T-403 (100/49 parts by weight), gelled for 16 h at 21 C and cured for 3 h at 80°C.

[b]Two-boss design.

Table 5. Winding pattern and fabrication data for titanium-lined Thornel Special graphite fiber/epoxy[a] vessels lined with 0.5-mm-thick titanium 6Al-4V (vessel volume a constant 0.965×10^{-3} m^3).

Data	All vessels	Vessel No.					
		CS-41	CS-42[b]	CS-43	CS-44	CS-45	CS-46
Composite Data							
Wall thickness, mm: hoop	0.74						
longitudinal	0.48						
Mass, kg: total vessel[c]		0.2392	0.2467	0.2423	0.2461	0.2479	0.2482
composite		0.0631	0.0747	0.0658	0.0653	0.0724	0.0730
fiber		0.0493	0.0516	0.0555	0.0552	0.0552	0.0546
one boss	0.0210						
adhesive coating	0.002 to 0.004						
Fiber content, vol%		70.5	69.0	78.3	78.9	68.2	66.6
Winding Data							
Longitudinal angle, deg	13						
Winding pattern	36-band, closed						
Hoop-to-longitudinal fiber ratio		1.75	1.94	1.94	1.94	1.94	1.94
Layers (interspersing): hoop	6 (2 + 4)						
longitudinal	4 (none)						
Total winding circuits: hoop		947	1047	1047	1047	1047	1047
longitudinal	1300						
Extra reinforcement	None						

[a]Epoxy resin system: XD 7818/T-403 (100/49 parts by weight), gelled for 16 h at 21°C and cured for 3 h at 80°C.
[b]No adhesive used to bond composite to liner.
[c]Two-boss design.

of 960 cycles). The titanium-lined vessels (Table 7) had an average cyclic life of 2190 cycles (low of 1780 cycles and high of 2540 cycles). Each of the fatigue failures was due to leakage caused by cracks in the metal liners. Leakage was easily detected by AE monitoring.

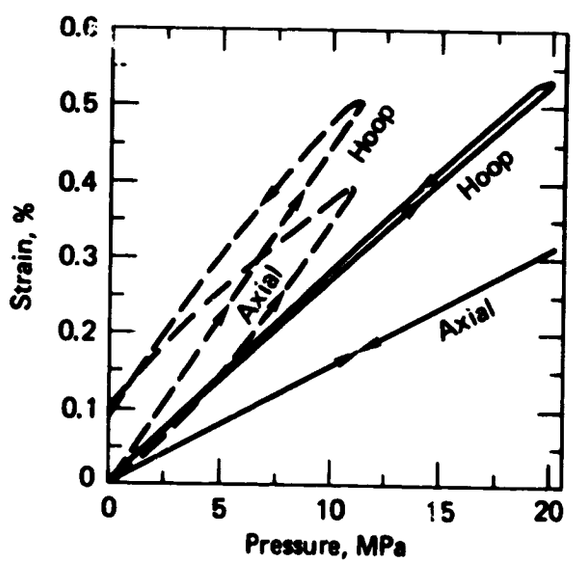

Fig. 11. Typical pressure vs strain curves during the first load cycle to 50% of the expected failure pressure of titanium-lined and aluminum-lined pressure vessels: solid curves denote titanium-lined vessel results, dashed curves denote aluminum-lined vessel results.

After these tests were completed, the vessels were cut in half for inspection. All of the cracks that led to the fatigue failures occurred in the center welds. Examination of the liner-to-composite adhesive bond indicated that this bond had retained its integrity during the cyclic testing of both the aluminum-lined and the titanium-lined vessels.

We were able to achieve an average cyclic life of more than 200 cycles in the titanium-lined vessels. the primary reason for this relatively high fatigue life is the high strength of the titanium bladder: i.e., during each cycle to the load level, the titanium liner underwent very little plastic deformation. The cyclic pressure vs strain curves in Fig. 11 show very little plastic deformation for the titanium-lined vessel. Conversely, Fig. 11 shows that there was substantial plastic deformation in the aluminum-lined vessel. In fact, because the aluminum-lined vessel did not load or unload elastically, the aluminum liner yielded both on pressurization and on depressurization. This same phenomenon is indicated in the pressure vs strain curves during the burst tests; Fig. 10 indicates by the change in slope that the titanium liner yielded at about 56% of the burst pressure whereas the aluminum liner yielded at about 20% of the burst pressure. Thus a low fatigue life for the aluminum-lined vessels must be expected.

Table 6. Burst pressure and cyclic fatigue for 5086 aluminum-lined Thornel Special graphite fiber/epoxy pressure vessels.

Data	Vessel No.					
	CS-36	CS-37	CS-38	CS-39	CS-40	CS-47[a]
Burst pressure, MPa	20.82	21.24	—	—	—	25.52
Fatigue life at 50% load level, cycles	—	—	55	372	960	—
Failure location[b]	F	F	W	W	W	F
Performance factor, TVM (TVM-1),[c] MPa·m³/kg	0.113 (0.121)	0.116 (0.124)	—	—	—	0.148 (0.161)
Strain at failure, %: hoop	—	—	—	—	—	0.98
axial	—	—	—	—	—	0.58
Strain at 50% load level, %: hoop	—	—	0.51	—	0.43	—
axial	—	—	0.40	—	0.37	—

[a]Winding difficulties; questionable test.

[b]F = fitting failure, W = weld failure.

[c]Performance factors based on total vessel mass (TVM) and total vessel mass minus the mass of one boss (TVM-1).

Qualitative correlation can be made between the present fatigue data and the fully reversed, uniaxial fatigue data for titanium and aluminum. Reference 8 gives a titanium (6Al-4V) fatigue life of about 1470 cycles, at the point where measurable plastic strain first appears during each cycle, and an aluminum (5456-H311) fatigue life of about 494 cycles, when appreciable plastic strain occurs during each cycle. An exact correlation of the present data and the data for uniaxial specimens is not possible primarily because it is very difficult to measure the significant strains in the liner-thickness direction during pressurization and depressurization.

The total vessel performance factor for the titanium-lined vessel is approximately the same as the maximum performance obtained for all-titanium vessels.[9]

Table 7. Burst pressure and cyclic fatigue for 6Al-4V titanium-lined Thornel Special graphite fiber/epoxy pressure vessels.

Data	Vessel No.					
	CS-41	CS-42[a]	CS-43	CS-44	CS-45	CS-46
Burst pressure, MPa	28.58	—	—	—	39.85	—
Fatigue life at 50% load level, cycles	—	1780	2540	2280	—	2230
Failure location[b]	H	W	W	W	F	W
Performance factor, TVM (TVM-1),[c] MPa·m³/kg	0.115 (0.126)	—	—	—	0.155 (0.170)	—
Strain at failure, %: hoop	—	—	—	—	1.22	—
axial	—	—	—	—	0.89	—
Strain at 50% load level, %: hoop	—	—	—	—	—	0.54
axial	—	—	—	—	—	0.32

[a]No adhesive used to bond composite to liner.

[b]H = hoop failure, F = fitting failure, W = weld failure.

[c]Performance factors based on total vessel mass (TVM) and total vessel mass minus the mass of one boss (TVM-1).

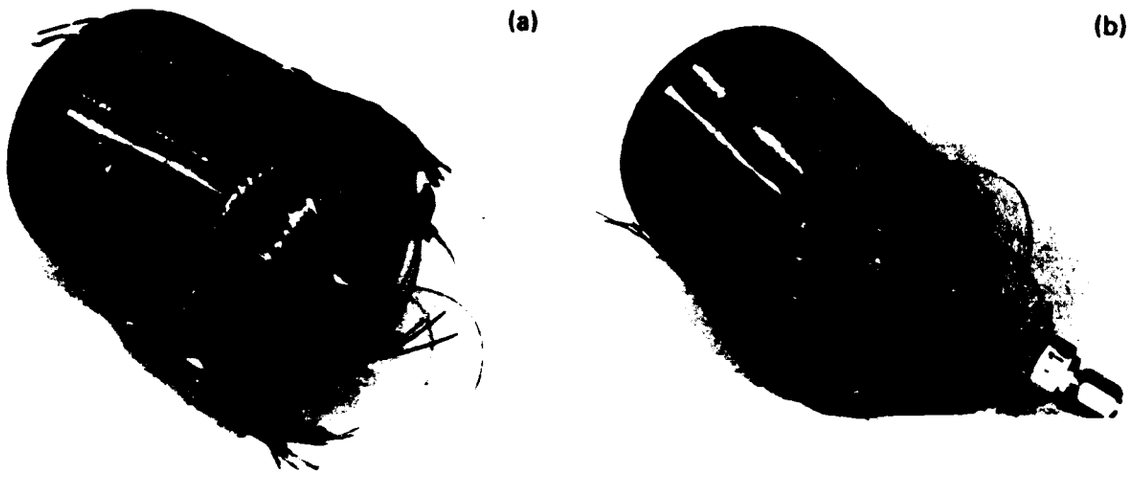

Fig. 12. Photograph of typical end failures during burst tests of titanium-lined (left) and aluminum-lined (right), Thornel Special graphite fiber/epoxy pressure vessels.

As is indicated in Table 7, this performance factor could be increased about 8% by replacing one boss with a dummy boss. A further increase in performance could be gained by improving our filament winding pattern to produce a balanced vessel (i.e., one with random failure locations). The current winding pattern, fixed after testing only one vessel, forced the burst failure to the fitting region (Fig. 12). in addition, some further gains in vessel performance may be possible with a better liner design. The limit to such improvements is somewhere below the composite performance factor given in Table 3 for an all-composite vessel (0.351 MPa·m^3/kg).

Ultrathin Titanium Liner[10]

An ultrathin titanium liner was tested in an attempt to improve the performance of the previous titanium-lined graphite/epoxy pressure vessels. The purpose of this work was threefold: (1) to halve the wall thickness of the titanium liner so that the vessel burst performance could be improved to at least 0.224 MPa·m^3/kg, (2) to develop a less costly liner fabrication method because machining full-size liners out of solid bar stock is prohibitively expensive, and (3) to determine the fatigue life of this ultrathin-titanium-lined vessel for cycling to 50% of the mean expected burst pressure.

Figure 13 is a schematic drawing of the finished 0.25-mm-thick titanium liner. In the manufacturing process, circular blanks were cut from 1.52-cm-thick 6Al-4V titanium plate. The circular blanks were then heated to about 941°C and held at that temperature for 12 to 15 min. By forcing the heated blanks through a lubricated die, we were able to forge elongated hemispherical blanks. These were air cooled, annealed for 1 h at 704°C, and then air cooled again. The hemispherical blanks were machined on a tape-controlled machine; just before making the final machine cuts, the liner halves were vacuum annealed following Mil-H.81200 A, Table IV. After the liner halves were electron-beam butt welded, each full liner was leak tested by pressurization to a level well below the point of plastic deformation. In addition, four liners were burst tested: the burst pressures were 5.58, 5.54, 5.50, and 5.53 MPa. All failures occurred as a result of axially oriented cracks in the cylindrical section of the liners.

Three sets of vessels were filament wound with the Thornel Special graphite fiber at a winding tension of 4.5 N. With the first set, successive changes were made in the winding pattern so we could determine which pattern produced maximum vessel performance. The second set of vessels was wound with a fixed winding pattern selected from the results of tests on the first vessel set. The third set of vessels was wound using the same fixed winding pattern on a redesigned titanium liner. The basic difference in the liner was a more gradual transition from the boss to the liner thickness (see Fig. 14). The winding tension was again 4.5 N. It was necessary to apply an increasing internal pressure (from 0.45 to 0.62 MPa) during the winding process and cure cycle to avoid collapsing the ultrathin liner. Details on the final winding pattern and the cure cycle are given in Table 8.

Testing and Results

For testing, the vessels were either pressurized with oil at a constant rate of 6.89 MPa/min until fail-

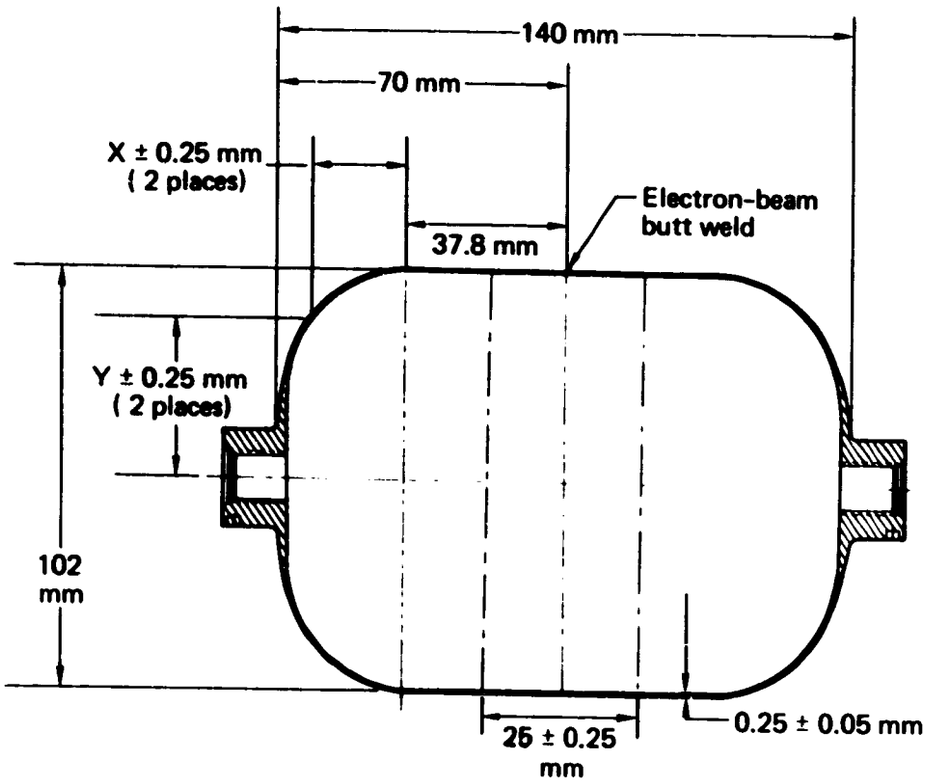

In-plane contour

Coordinates	
X	Y
0.00	50.80
3.48	50.55
7.75	49.58
11.84	47.98
18.92	42.90
21.87	38.65
24.36	36.07
26.37	32.18
27.99	28.12
29.18	23.88

Fig. 13. Design of the 10.2-cm-diameter titanium alloy (6Al-4V) liner.

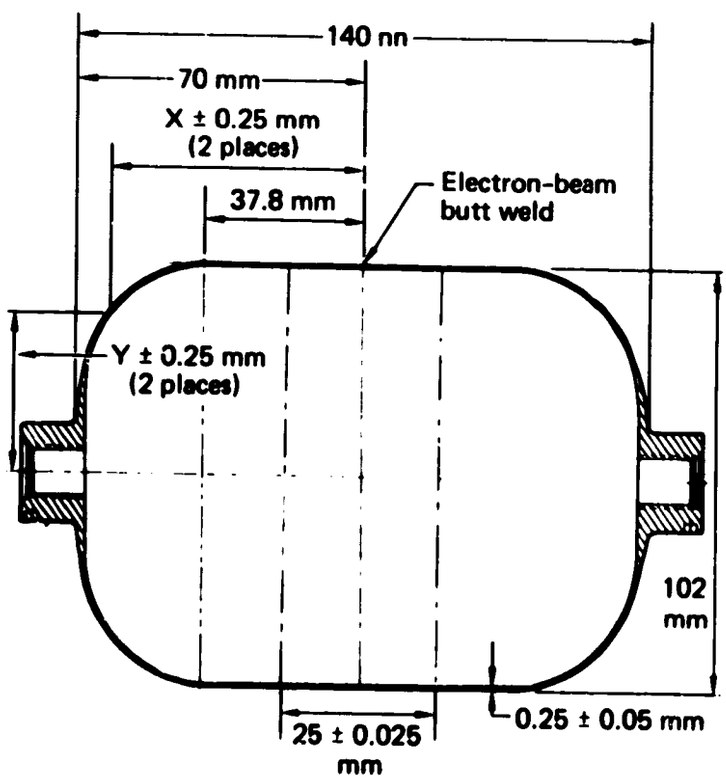

Outer contour

Coordinates	
X	Y
0.00	50.80
7.29	50.80
14.91	50.80
22.53	50.80
35.23	50.80
41.22	50.52
49.58	47.96
59.64	39.65
64.14	32.18
66.93	23.85
67.95	19.05
69.16	12.70
69.67	10.16

Inner contour

Coordinates	
X	Y
0.00	50.55
7.29	50.55
14.91	50.55
25.07	50.55
35.26	50.55
41.15	50.22
49.95	47.70
59.44	39.52
63.88	32.05
66.62	22.86
67.92	12.20
68.07	8.89

Fig. 14. Redesigned titanium alloy liner.

Table 8. Final winding pattern and test results for the ultrathin, (set 1): titanium-lined Thornel Special graphite fiber/epoxy[a] pressure vessels: liner thickness = 0.25 mm, test temperature = 23°C.

Data	Mean	Vessel No. T-13	T-14	T-15	T-16	T-17	T-18
Vessel Data							
Volume, 10^{-4} m^3	9.625						
Burst pressure, MPa	47.49	47.13	50.33	50.33	46.62	48.95	41.78
Failure location[b]		F	F	F	F	F	H
Performance factor,							
MPa·m^3/kg: composite	0.406	0.384	0.435	0.438	0.397	0.428	0.357
total vessel	0.241	0.233	0.256	0.258	0.235	0.251	0.215
Composite Data							
Mass, kg: total vessel[b, c]	0.189	0.1945	0.189	0.1881	0.1899	0.1875	0.1874
composite	0.112	0.1185	0.1114	0.1107	0.1125	0.1105	0.1126
fiber	0.088	0.0889	0.0876	0.0889	0.0899	0.0892	0.0862
Fiber content, vol%	71.5	67.3	71.5	73.5	73.0	74.4	69.0
Vessel wall thickness,							
mm: hoop	2.76						
longitudinal	1.32						
Winding Data							
Longitudinal angle, deg (min)	10(3)						
Winding pattern	36-band, closed						
Layers (interspersing): hoop	8(2+6)	8(2+6)	8(2+6)	8(2+6)	8(2+6)	8(2+6)	8(2+6)
longitudinal	6(none)	6(none)	6(none)	6(none)	6(none)	6(none)	6(none)
Total winding circuits: hoop	1600	1600	1600	1600	1600	1600	1600
longitudinal	1728	1728	1728	1728	1728	1728	1728

[a]Epoxy resin system: XD 7818/T-403 (100/49 parts by weight), gelled for 16 h at 40°C and cured for 3 h at 80°C.

[b]H = hoop failure, F = fitting failure.

[c]Includes typical weights: mandrel = 76.5 g (including total boss weight of 13.6 g), adhesive = 2.1 g, Kevlar 49 support rings = 0.4 g (see Table 7 notes).

ure, or sinusoidally cycled at a rate of 0.66 Hz between 0+ and 50% of their expected burst pressure. After three of the first four vessels tested failed by leakage and could not be burst, we examined the liners and discovered that during pressurization, small cracks had developed from a stress concentration located at the transition from the liner thickness to the boss.

To obtain a failure by burst, the boss ends of the insides of subsequent vessels were coated with a flexible epoxy (Mereco 4051). Coating the ends also enabled the vessels wound with the final winding pattern to withstand a substantial number of fatigue cycles before the cracks in the vessel ends propagated beyond the coated region. These early tests indicated that the fatigue life of the weld region was at least 2000 cycles at the 50% load level, well beyond the NASA Space Shuttle requirements.

Table 9 gives burst pressures and fatigue lives for the optimal winding pattern (second set of vessels); Table 10 gives burst performance for one vessel and fatigue lives for six vessels wound with the final fixed winding pattern and the redesigned liner (third set of vessels). For all of the vessels with the stress concentration (sets one and two) except one, leakage failure occurred because of end cracks propagating beyond the coated region. Leakage failure in the one exceptional case caused by a fatigue crack in the weld region (vessel A, 4000 cycles at about 50% expected burst pressure). All the fatigue tested vessels in the third set experienced leakage failure resulting from a fatigue rack in the weld region. Figure 15 shows typical axial

Table 9. Cyclic fatigue life of the second set of vessels, those with the fixed winding pattern.

Vessel No.[a]	Cyclic life,[b, c] cycles
T-19	3140
T-20	2020
T-21	3050
T-22	1935[d]
T-23	1935
T-24	3485
T-25	2720

[a]Vessel fabrication identical to that of T-13 and T-18 of set 1.

[b]Four cycles per minute, 1 to 50% of expected burst pressure.

[c]In all cases, vessel leakage resulted from propagation of end cracks beyond the coated region.

[d]Minimum value; chart recorder stuck.

Table 10. Burst performance and cyclic fatigue life of the third set of vessels, those with the redesigned titanium liner.

Vessel No.[a, b]	Burst performance, kPa·m³/kg	Cyclic life,[c] cycles
T-26	—	8400
T-27	—	1600
T-28	—	1186
T-29	—	1650
T-30	236	—
T-31	—	600
T-32	—	402

[a]All vessels were wound as described in Table 8. The redesigned mandrel weighed more, increasing the total vessel weight by about 5% over that reported in Table 8.

[b]All vessels except T-26 had welds with incomplete penetration.

[c]Four cycles per minute, 1 to 50% of expected burst pressure.

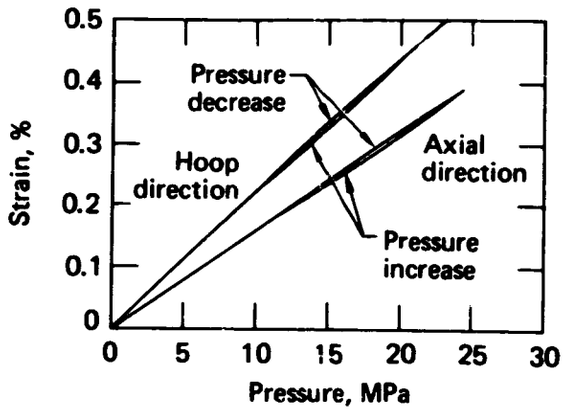

Fig. 16. Typical axial and hoop strains on the outer surface of the fiber/epoxy composite in the cylindrical portion of the vessel during the first load cycle to 50% of the expected burst pressure.

and hoop strains for burst tested vessels wound with the final fixed winding pattern. In the fatigue tests, vessel leakage was determined by AE monitoring.

Discussion

We were able to achieve a mean total vessel burst performance of 0.241 MPa·m³/kg for small metal-lined vessels in which the two bosses comprised about 7% of the total vessel weight (see Table 8). As a comparison, Ref. 11 presents data for spherical, titanium-lined Kevlar 49 vessels for which a maximum total vessel burst performance of 0.189 MPa·m³/kg was achieved. Reference 12 provides data for spherical, stainless-steel-lined Kevlar 49 vessels: a maximum total vessel burst performance of 0.202 MPa·m³/kg was obtained. The corresponding maximum performance achieved in our present work is 0.258 MPa·m³/kg. Thus, in terms of burst performance, our titanium-lined graphite/epoxy system is some 30% better than these reported Kevlar 49 systems.

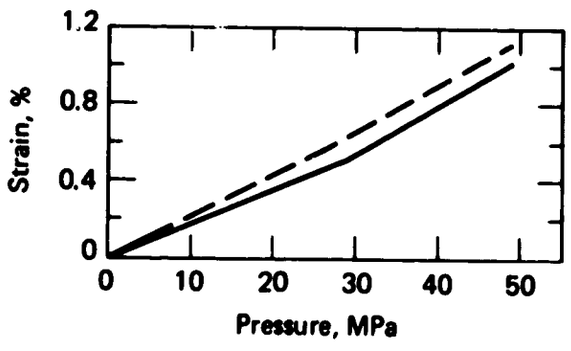

Fig. 15. Typical axial (solid curve) and hoop (dashed curve) strains on the outer surfaces of the fiber/epoxy composite in the cylindrical portion of the vessel.

Furthermore, the axial and hoop failure strains in the graphite-overwrapped vessel are only approximately 1.2%, compared with 1.8% in the Kevlar-overwrapped vessel. Thus, the fatigue life of the graphite vessel should be significantly greater than that of the Kevlar vessel because, as observed previously, smaller strain changes during each cycle tend to increase the fatigue life of the liner.

The redesigned liner (used in the third set of vessels) successfully solved the problem of the stress concentration at the ends of the titanium liners. Thus, it was no longer necessary to coat the inner ends of these vessels with epoxy. The redesigned liner was slightly heavier, however, resulting in an increase in total vessel weight of about 5%. During the fatigue tests of the third set of vessels, all failures resulted from cracks in the welds. Figure 16 plots the cyclic strains during the first fatigue cycle for a typical vessel wound over this redesigned liner.

Unfortunately, after the first vessel was welded with the same weld parameters as were used with the first two sets, difficulties were encountered. Specifically, the welding process "burned" a couple of small holes through the second vessel. Therefore, cooler welds were used for the remaining vessels in the third set. However, this change created another problem. The remaining vessels in this set were found to be defective, having welds with incomplete penetration (see Fig. 17a). Thus, except for vessel T-26, the first one in this set, the vessel fatigue lives at the 50% load level were low (see Table 9).

Because of the liner problems (stress concentrations and incomplete weld pentration), careful study of the fatigue data will be required to determine correctly the fatigue life of a "normal" vessel (see Fig. 17b). The one test vessel free from both liner problems

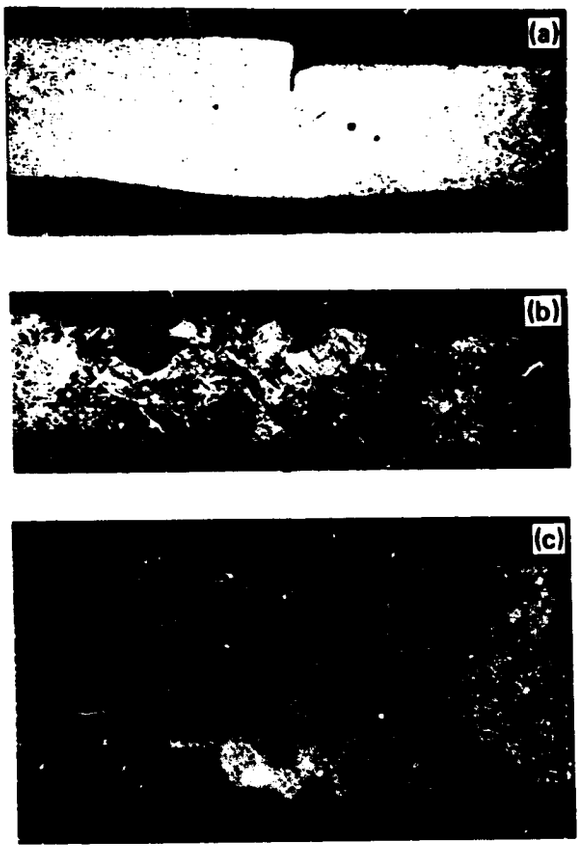

Fig. 17. Photomicrographs of electron-beam butt welds: (a) poor weld in a 0.25-mm-thick liner, (b) good weld in a 0.25-mm-thick liner, (c) good weld in a 0.51-mm-thick liner.

had a fatigue life of 8400 cycles at the 50% load level. All of the vessels in the first two sets had "good" welds, but because the end cracks propagated out of the coated region before any weld cracks formed, these fatigue data only give a lower bound on the weld fatigue life. On the basis of data from eight different vessels, this lower bound is somewhere between 1935 and 3485 cycles. The one vessel in the first set that leaked from a crack in the weld region (not from an end crack) lasted 4000 cycles. Thus, it appears that the minimum fatigue life of the ultrathin-titanium-lined vessels meeting both conditions (no stress concentration and "good" welds) is greater than 2000 cycles and could be as high as 4000 cycles.

The relatively high fatigue life of the weld region is surprising in view of past experience. Because the titanium liner used in this study is only half as thick as the liner used in the previous work, one would expect that the plastic strain change per cycle would be greater in the ultrathin liners and that the fatigue life of the weld region thus would be lower. The photomicrographs in Figs. 17b and 17c reveal why the welds in the ultrathin liners have better fatigue lives, even though the welds in the previous liners were twice as thick. In the thick-liner weld (Fig. 17c), there are more geometric discontinuities in the form of notches and weld-bead drop-throughs. The ultra-thin-liner weld (Fig. 17b) is not nearly as V-shaped and therefore the transition from the cast weld material to the parent liner material is not as distinct. These factors all serve to reduce the stress concentrations on the ultrathin-liner weld and produce a longer fatigue life.

Conclusions

From the above described studies of graphite fiber and the ultrathin metal liners for composite pressure vessels, we draw the following conclusions:

- The Thornel Special graphite fiber in an epoxy matrix has a modulus of 206 GPa, a rupture tensile stress of 3570 MPa, and a rupture strain of 1.7%. The fiber tensile properties are not affected by liquid nitrogen temperature or by various quasi-static strain rates. The data scatter, however, is on the undesirably high side.
- For long-term, tensile-critical applications where composite density also is a key consideration, we consider the Thornel Special graphite fiber to be one of the best fibers for composites.
- For applications where the environment is hostile and where shear and compression stresses also are present, the Thornel Special graphite fiber is one of the most attractive fibers that can be made commercially available. However, the quality consistency (i.e., large CV) of the fiber must be improved before this fiber can become an acceptable engineering material.
- The average composite performance factor for the Thornel Special graphite fiber/epoxy cylindrical pressure vessel was determined to be 0.351 $MPa \cdot m^3/kg$. Because of its greater yield strength, a titanium-lined graphite fiber/epoxy pressure vessel was found to have substantially better fatigue life (for cycling to 50% of the expected burst pressure) than an aluminum-lined vessel. The present aluminum-lined graphite fiber/epoxy vessel cannot meet the 1000-fatigue-cycle requirement. The total vessel performance factor for a 0.5-mm-thick titanium-lined graphite fiber/epoxy vessel was found to be 0.155 $MPa \cdot m^3/kg$. This vessel design does meet the fatigue life requirement and can be used to contain both nitrogen gas and helium for aerospace applications.
- The ultrathin (0.25-mm-wall thickness) 6Al-4V titanium-liners for graphite fiber/epoxy vessels were manufactured from flat plate. Very high total

vessel burst performance was achieved: the mean burst performance was 0.241 MPa·m³/kg. The data indicate that where "good" welds are made, liner fatigue lives in excess of 2000 to 3000 cycles can be obtained for cycling to 50% of the expected burst pressure.

References

1. T. T. Chiao, M. A. Hamstad, and E. S. Jessop, "Tensile Properties of an Ultrahigh-Strength Graphite Fiber in an Epoxy Matrix," presented at *ASTM Conf. Composite Reliability*, April 15-16, 1974, Las Vegas, NV.
2. T. T. Chiao and R. L. Moore, "A Room-Temperature-Curable Epoxy for Advanced Fiber Composites," in *Proc. SPI Reinforced Plastics/Composites Institute, 29th Ann. Tech. Management Conf.*, February 5-8, 1974, Washington, D.C.
3. T. T. Chiao, R. L. Moore, and C. M. Walkup, "Graphite Fiber/Epoxy Composites," *SAMPE Quart.* 4(4), 7 (1973).
4. T. T. Chiao and R. L. Moore, "Tensile Properties of PRD-49 Fiber in Epoxy Matrix," *J. Composite Mat.* **6**, 547 (1972).
5. T. T. Chiao and R. L. Moore, "Strain Rate Effect on the Ultimate Tensile Stress of Fiber/Epoxy Strands," *J. Composite Mat.* **5**, 124 (1971).
6. M. A. Hamstad, T. T. Chiao, and R. G. Patterson, "Fatigue Performance of Metal-Lined Graphite/Epoxy Pressure Vessels," *Composites* **6**, 249 (1975); see also Lawrence Livermore Laboratory, Preprint UCRL-75759 (1974).
7. T. T. Chiao, R. L. Moore, and C. M. Walkup, *Graphite Fiber/Epoxy Composites*, Lawrence Livermore Laboratory, Rept. UCRL 74579 (1973).
8. R. W. Smith, M. H. Hirschberg, and S. S. Manson, *Fatigue Behavior of Materials Under Strain Cycling in Low and Intermediate Life Range*, National Aeronautics and Space Administration, Rept. NASA-TN-D-1574 (1963).
9. *Aerospace Tanks: Characteristics of Existing Propellant Tanks and Pressure Vessels for Spacecraft Applications*, National Aeronautics and Space Administration, IIT Research Institute, Chicago, IL, Repts. NASA-CR-104101, Vol I, and NASA-CR-104100, Vol II (1969).
10. M. A. Hamstad and T. T. Chiao, "Graphite/Epoxy Pressure Vessels Lined with Ultrathin Titanium," in *Proc. 22nd Natl. SAMPE Symp.*, April 26-28, 1977, San Diego, CA.
11. W. W. Schmidt, *Development of High Efficiency Space Shuttle Tankage*, Brunswick Corporation, Lincoln NB (1976).
12. R. E. Landes, *Test Evaluation of Overwrapped Pressure Vessels, Contract NAS 3-16770* Structural Composites Industries, Inc., Azusa, CA, Quarterly Technical Progress Narrative No. 11 (30 December 1974 to 30 March 1975).

PART II. EPOXY MATRICES FOR FILAMENT WOUND KEVLAR 49/ EPOXY PRESSURE VESSELS

Screening of Epoxy Systems[13]

Purpose

The epoxy resin systems used in many high-performance filament wound pressure vessels and rocket motor cases have been based on the diglycidyl ether of bisphenol A (DGEBA), diluted with bis(2,3-epoxycyclopentyl)ether (such as ERL 2256 from Union Carbide Corporation) and cured with mixed aromatic amines.[14] These systems are quite attractive for filament winding, both for their tensile properties and for their processing characteristics. However the diluent, bis-(2,3-epoxycyclopentyl)ether, is no longer commercially available and alternate epoxy systems must be sought for the wet filament winding process.

Ideally, the way to select an epoxy system is to understand thoroughly all those matrix properties that contribute to high performance in the filament wound structure and then select an epoxy resin system that maximizes the desirable properties. Unfortunately, this is not possible because credible data even of neat resin properties are not plentiful. Intuitively, the viscosity, wetting properties, and adhesion characteristics of the neat resin; the tensile strength, modulus, and elongation of the cured resin, as well as the cure temperature and resin shrinkage during cure are believed to have an effect on the performance of the final composite structure. The relative importance of each has not been clearly established.

We have been investigating the effect of resin properties on the burst strength of the filament wound structure. Our method for selecting a new epoxy system is to examine neat resins that closely resemble the systems containing the bis(2,3-epoxycyclopentyl)-ether in processing characteristics and tensile properties. Although this method may not identify the best resin systems for filament wound vessels, it does ensure that the selected resin systems will meet certain essential requirements at the outset. We need to develop epoxy resins to meet two pot life requirements, one where processing does not require a long pot life (for small filament wound vessels) and another where a very long pot life is needed (for large filament wound parts).

In this study of resin systems, we looked for tensile properties similar to those of selected reference systems and for easy processing in the uncured resin. The results of our overall screening of several promising systems are summarized below. Viscosities, gel times, and cast resin tensile behavior were determined to guide our selection of a few systems for more extensive tests in filament wound structures. In addition, data on heat deflection under load and water absorption measurements were gathered for comparative purposes and for screening where special operating environments are a consideration.

Test Epoxy Resin Systems

The resin used in most of our formulations was the diglycidyl ether of bisphenol F (DGEBF), the bisphenol formed from phenol and formaldehyde. This resin is similar to the earlier epoxy resins based on DGEBA but has a lower viscosity (3.4 Pa·s at 25°C) and gives slightly higher tensile properties. A typical commercial product is XD 7818 epoxy from Dow Chemical Company.

In some of the test formulations, we used DGEBA plus ≈10 wt% of a carboxy-terminated butadiene-acrylonitrile copolymer (CTBN). This copolymer was added to improve the fracture toughness of the cured resin.[15] A typical commercial product is the XD 7575.02 epoxy from Dow Chemical Company.

Two diluents were used to lower the viscosity of the epoxy systems; vinylcyclohexene dioxide (VCHDO) and the diglycidyl ether of neopentylglycol. Typical commercial products are, respectively, Union Carbide Corporation's ERL 4206 and Dow Chemical Company's XD 7114.

Aromatic amines were used as curing agents. These included Tonox 60-40, Tonox LC, and 2,6-diaminopyridine (DAP), all from Uniroyal. Tonox 60-40, a liquid at room temperature, is a mixture of 60% crude methylene dianiline and 40% metaphenylene diamine. Tonox LC is similar to crude methylene dianiline but is made by reacting formaldehyde with aniline plus another aromatic amine to break up the crystallinity in the final product. Tonox LC reacts with epoxies more slowly than Tonox 60-40. The 2,6-DAP, a powder at room temperature, gives cure properties similar to metaphenylene diamine but reacts considerably slower with epoxies.

For the reference resins, we selected three epoxy systems. Two of the systems have been used widely for filament winding but are no longer available. They consist of liquid DGEBA resins (ERL 2256 and ERL 2258 from Union Carbide) diluted to different viscosities with bis(2,3-epoxycyclopentyl)ether. The third reference resin is a low-viscosity liquid DGEBA resin (Shell Chemical Company's Epon 826), diluted with the crude diglycidyl ether of 1,4-butanediol (Ciba-Geigy's RD-2).[16] The curing agents used in the refer-

ence resin systems were either Tonox 60-40 or a mixture of methylene dianiline and metaphenylene diamine that was reacted with a small amount of DGEBA resin (Union Carbide's ZZL 0820).

Test Methods. Tensile test specimens were prepared from resin sheets that were cast between glass plates. The mold was formed with rubber tubing (as a dam), precision spacers, and clamps.[17] Individual 3.2-mm-thick specimens were prepared according to ASTM D638 Type I. Great care was taken to smooth and polish the machined surfaces. The specimens were tested on a universal tensile test machine at a crosshead speed of 5 mm/min.

Viscosity measurements were made with a Brookfield rotating-spindle viscosimeter (Model LVT) using a No. 1 spindle in a temperature-controlled bath (25°C). A 300-g aliquot of the resin mixture in a glass container (5.5 mm in diameter) was brought to temperature (±0.2°C) and tested within 1 h after mixing.

Gel times were determined on a 30-g sample. The sample was placed in a 2.5-cm diameter test tube that was immersed in a constant-temperature bath at 25°C. A gel timer repeatedly dropped a 6-g weight into the sample and then pulled it out. Gel time is defined as the point at which the viscosity of the sample is great enough to support the 6-g weight for 15 s.

Results and Discussion. For applications where a pot life of under 40 h (for a 30-g mass) is acceptable, new resins were formulated by selecting the combination of resins and diluents that, when mixed with the stoichiometric amount of curing agent, gave a viscosity in the desirable range from 0.7 to 0.9 Pa·s at 25°C. These resin systems and their viscosities, gel times, tensile properties, and heat distortion temperatures are shown in Table 11. The corresponding tensile stress-strain curves are shown in Fig. 18.

For applications where a pot life of over 40 h (for a 30-g mass) is needed, new resins were formulated from the base resin-diluent combination that gave the desired viscosity when mixed with the stoichiometric amount of curing agent. The longer pot lives are obtained by modifying the curing agent, i.e., using Tonox 60-40 with an equal amount of either 2,6-DAP or Tonox LC. These formulations and their viscosities, gel times, tensile properties, and heat distortion temperatures are shown in Table 12. The corresponding tensile stress-strain curves are plotted in Fig. 19. For comparison, the properties of the reference epoxy systems are listed in Table 13 and their tensile behavior is plotted in Fig. 20.

An examination of Table 11 and Fig. 18 against Table 13 and Fig. 20 indicates that formulations 2 and 4 are the most promising resin systems for filament winding where a very long pot life is not a key requirement. These two new epoxy systems more than match the reference systems in tensile strength and come close to the desired elongation and modulus. The water absorption characteristics of these new systems are superior to that of the reference epoxies. Formulations 2 and 4 do have lower heat distortion temperatures than the reference systems but these possibly can be improved with a high cure temperature.

Table 11. Properties of epoxy systems with moderate pot lives.

Property	System 1	System 2	System 3	System 4
Resin components (parts by weight)	XD 7818/XD Tonox 60-40 (100/30/31.5)	XD 7818/ERL 4206/ Tonox 60-40 (100/30/39.7)	XD 7818/XD 7575.02/ XD 7114/Tonox 60-40 (50/50/45/33.7)	XD 7818/XD 7575.02/ ERL 4206/Tonox 60-40 (50/50/30/38.1)
Cure cycle, h/°C	4/60 + 3/120	4/60 + 3/120	4.5/60 + 3/120	4.5/60 + 3/120
Gel time for a 30-g mass at 25°C, h	26	30	30	40
Viscosity at 25°C, Pa·s	0.80	0.90	0.80	0.70
Number of specimens tested	8	6	8	6
Tensile properties: Maximum stress, MPa (CV, %)	95.3 (0.4)	116.9 (0.7)	87.9 (0.3)	110.7 (0.4)
Strain at maximum Stress, % (CV, %)	6.5 (2.3)	6.1 (7.0)	6.1 (1.4)	6.2 (5.6)
Secant modulus at 0.01 strain, MPa (CV, %)	2944 (5.9)	3425 (3.0)	2960 (0.8)	3328 (1.4)
Heat distortion temperature, °C	100	118	100	128
Water absorption after 6 h in boiling water, % gain	1.95	1.10	1.42	1.13

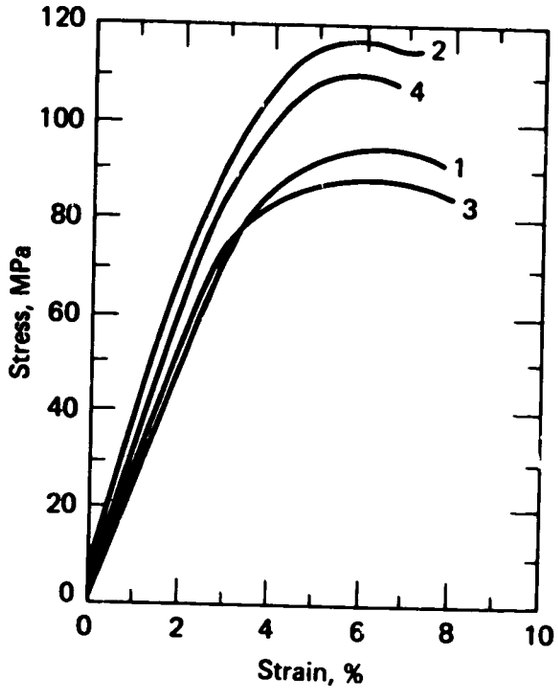

Fig. 18. Tensile properties of the epoxy systems with relatively short pot lives: (1) XD 7818/XD 7114/Tonox 60-40, (2) XD 7818/ERL 4206/Tonox 60-40, (3) XD 7818/XD 7575.02/XD 7114/Tonox 60-40, and (4) XD 7818/XD 7575.02/ERL 4206/Tonox 60-40.

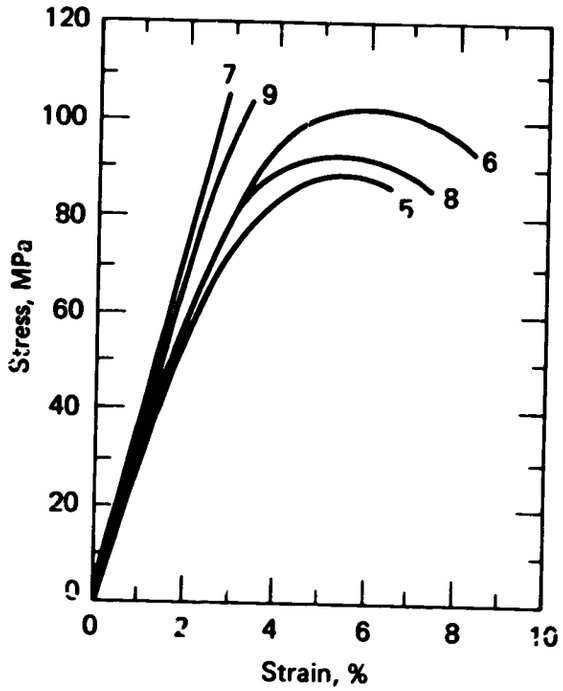

Fig. 19. Tensile properties of epoxy systems with long pot lives: (5) XD 7818/XD 7114/Tonox LC, (6) XD 7818/XD 7114/Tonox 60-40/DAP, (7) XD 7818/ERL 4206/Tonox 60-40/DAP, (8) XD 7818/XD 7575.02/XD 7114/Tonox 60-40/ DAP, and (9) XD 7818/XD 7575.02/ERL 4206/Tonox 60-40/DAP.

Table 12. Properties of epoxy systems with long pot lives.

Property	System 5	System 6	System 7	System 8	System 9
Resin components (parts by weight)	XD 7818/ XD 7114/ Tonox LC (100/45/50.3)	XD 7818/ XD 7114/ Tonox 60-40/ 2,6-DAP (100/30/13.2/13.2)	XD 7818/ ERL 4206/ Tonox 60-40/ 2,6-DAP (100/20/14.4/14.4)	XD 7818/ XD 7575.02/ XD 7114/ Tonox 60-40/ 2,6-DAP (50/50/45/14.1/14.1)	XD 7818/ XD 7575.02/ ERL 4206/ Tonox 60-40/ 2,6-DAP (50/50/30/15.9/15.9)
Cure cycle, h/°C	5/60 + 3/120	5/60 + 3/120	5/80 + 3/120	5/80 + 3/120	5/80 + 3/120
Gel time for a 30-g mass at 25°C, h	57	71	95	90	109
Viscosity at 25°C, Pa·s	0.85	0.85	0.80	0.85	0.80
Number of specimens tested	7	7	6	8	6
Tensile properties:					
Maximum stress, MPa (CV, %)	90.0 (0.7)	101.5 (0.1)	102.8 (4.2)	93.1 (0.1)	102.5 (1.6)
Strain at maximum stress, % (CV, %)	5.3 (2.6)	5.8 (2.3)	3.1 (6.8)	5.3 (1.6)	3.6 (2.2)
Secant modulus at 0.01 strain, MPa (CV, %)	3061 (3.5)	3157 (3.2)	3917 (1.5)	3195 (2.6)	3799 (2.3)
Heat distortion temperature, °C	82	97	106	89	112
Water absorption after 6 h in boiling water, % gain	1.43	1.60	1.52	2.20	1.14

Table 13. Properties of the reference epoxy systems.

Property	System 10	System 11	System 12
Resin components (parts by weight)	ERL 2256/Tonox 60-40 (100/29.5)	ERL 2258/ZZL 0820 (100/31)	Epon 826/RD-2/Tonox 60-40 (100/25/28.3)
Cure cycle, h/°C	16/50 + 2/95 + 3/150	16/60 + 3/160	3/60 + 2/120
Gel time for a 30-g mass at 25°C, h	41	30	23
Viscosity at 25°C, Pa·s	1.59	1.40	1.20
Number of specimens tested	7	7	8
Tensile properties:			
Maximum stress, MPa (CV, %)	107.5 (0.4)	107.2 (1.9)	89.6 (0.3)
Strain at maximum stress, % (CV, %)	7.1 (5.3)	5.2 (6.4)	7.8 (3.0)
Secant modulus at 0.01 strain, MPa (CV, %)	3460 (2.4)	3736 (2.3)	2683 (3.6)
Heat distortion temperature, °C	133	152	121
Water absorption after 6 h in boiling water, % gain	1.45	1.78	0.93

A comparison of the data on the long-pot-life epoxy systems (Table 12 and Fig. 19) with the reference systems data (Table 13 and Fig. 20) indicates that the formulations with the diglycidyl either of neopentylglycol have the best elongation. Formulation 6 exhibits the best balance of properties. The formulations containing both VCHDO and 2,6-DAP have good tensile strengths but exhibit low elongations, probably because of a combination of the very rigid, cyclic structure of 2,6-DAP with the less rigid, cyclic structure of VCHDO.

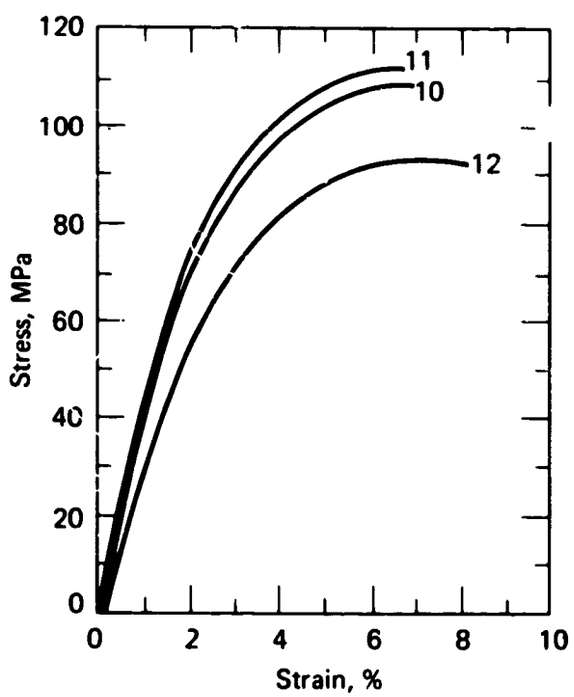

Fig. 20. Tensile properties of the reference epoxy systems: (10) ERL 2256/Tonox 60-40, (11) ERL 2258/ZZL 0820, and (12) Epon 826/RD-2/Tonox 60-40.

Surprisingly, the heat distortion temperatures shown in Tables 10 and 12 are not consistent with our expectations. For example, formulation 4 (Table 11) contains approximately 5% rubber but has a heat distortion temperature 9°C higher than that of formulation 2 that lacks the rubber component. We do not know how to explain this.

Filament Wound Pressure Vessels of Kevlar 49 Fiber in Several Epoxy Matrices[18]

Purpose

Our next objective was to select the best epoxy from the previously screened systems. Because the resins used in this study do not differ widely in mechanical properties, we did not attempt to differentiate the epoxy systems by evaluating the effect of resin properties on the performance of filament wound vessels. In selecting an epoxy system for high-performance filament winding applications, we determined that the

epoxy must have passed the previously described screening step and still be acceptable (although not necessarily the best) in terms of vessel performance. We did not use vessel performance as the most important criterion because we doubt that the burst test is the fairest or most effective method of judging matrix performance. For example, a high-burst-performance epoxy may very possibly have a low heat distortion temperature that renders the system unacceptable for the intended application.

Fiber/Epoxy Strand Specimens

For the reinforcing fiber, we selected DuPont's Kevlar 49, a high-modulus, high-strength organic fiber of poly(p-phenylene terephthalamide). We used five spools of 380-denier, 267-filament Kevlar fiber, dried before winding for 70 h at 50°C under 13.3 Pa pressure. The average cross-sectional area determined from 48 specimens of the single fiber strand (calculated from the manufacturer's fiber density and our fiber weight measurements) is 2.93×10^{-8} m^2 with a CV of 1.5%.

We used epoxy-impregnated fiber strands (Fig. 21) to characterize the unidirectional breaking strength of the Kevlar 49 fiber. The strands were fabricated by vacuum epoxy-impregnation on a numerically controlled winding machine at a winding tension of 4.4 N. We tested 25.4-cm-gage length strand specimens at a machine cross-head speed of 1 cm/min: Table 14 summarizes these data.

Filament Wound Pressure Vessels

We wound the epoxy-impregnated Kevlar 49 fiber over a water-soluble type of mandrel coated with a 0.5-mm-thick chlorobutyl rubber coating. This rubber coating becomes the liner of the vessel when the mandrel is washed away with hot water. The cylindrical vessel had a diameter of 10.2 cm, a vessel length-to-diameter ratio of 1.4, and a boss diameter-to-vessel diameter ratio of 0.16 (Fig. 22). We used the "in-plane" dome contour based on ASTM D-2585-68. The axial winding angle was 10 deg, 13 min. The hoop-to-axial fiber ratio, in terms of winding circuits, was 1.5. This slightly unbalanced design forces failure into the hoop winding direction.

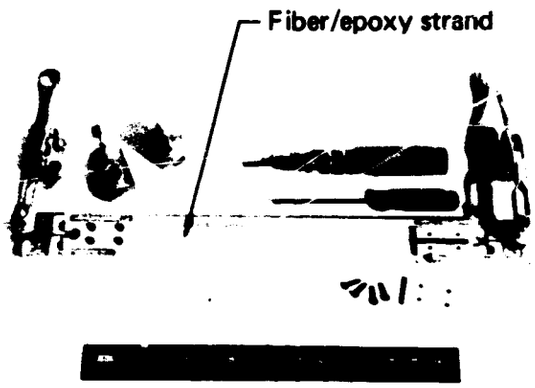

Fig. 21. Clamping arrangement for testing the fiber strengths of epoxy-impregnated strands.

The vessels were also fabricated on the numerically controlled winding machine which was equipped with a vacuum impregnation chamber. Only the fiber spool and the impregnation apparatus were placed inside the vacuum chamber (maintained at 670 Pa).

Table 14. Fiber strength of fiber strands impregnated with various epoxy resins.

Epoxy system No.	No. of strand specimens[a]	Fiber content, vol%	Fiber Tensile Properties[b]		
			Rupture stress, MPa	Rupture strain, %	Rupture modulus, GPa
Moderate Pot Life Epoxy Systems					
2	44	63.5	3612 ± 32	2.6 ± 0.01	137.2 ± 0.6
3	9	61.0	3447 ± 110	2.6 ± 0.10	132.4 ± 1.2
4	68	62.5	3378 ± 32	2.4 ± 0.03	141.3 ± 0.8
Long Pot Life Epoxy Systems					
5	30	65.1	3461 ± 52	2.6 ± 0.03	134.4 ± 0.6
6	29	64.6	3247 ± 56	2.3 ± 0.04	143.4 ± 0.7
8	43	65.1	3302 ± 12	2.4 ± 0.02	139.9 ± 0.9
Reference Epoxy Systems					
10	48	61.3	3543 ± 27	2.6 ± 0.05	137.9 ± 1.6
11	24	62.4	3578 ± 100	2.6 ± 0.03	137.9 ± 2.3
12	22	63.6	3468 ± 43	2.6 ± 0.01	135.1 ± 0.2

[a] These data represent five spools of yarn. The test strands were taken on a daily basis during the vessel winding.

[b] For each resin system, CV = 7%, nominally 4.5%.

[c] The ± values are the 95% confidence limits.

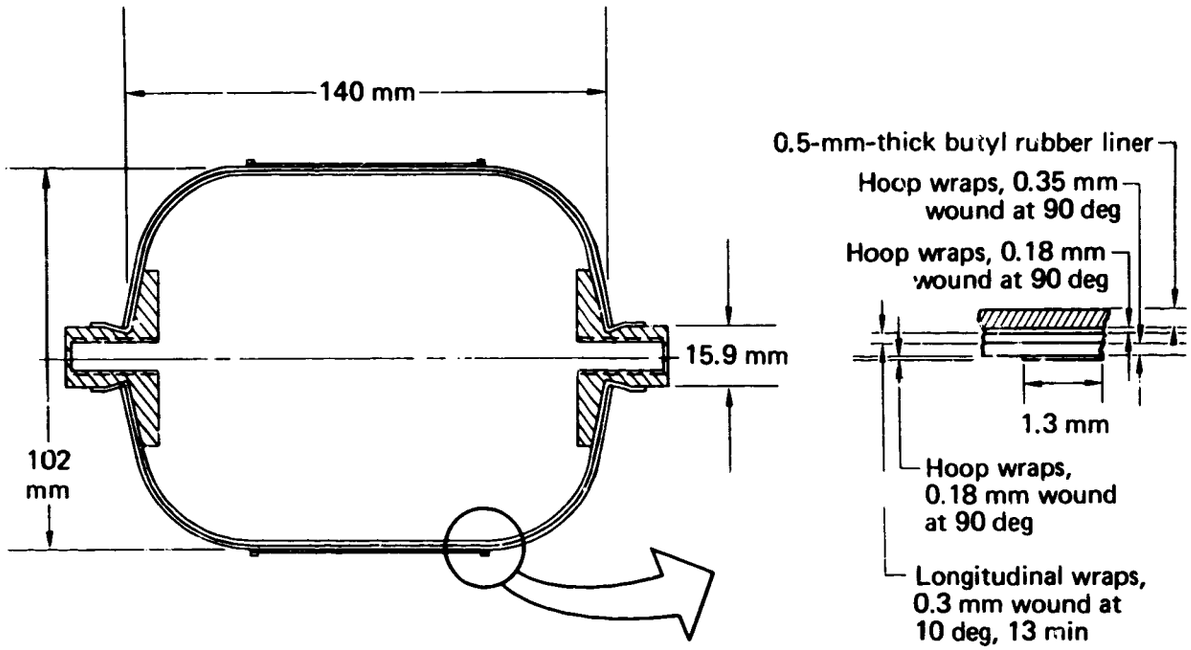

Fig. 22. Design of the pressure vessel used to test the various epoxy systems.

For the 380-denier yarn, we used a 4.4-N winding tension (Fig. 22). Normally, we fabricated strand specimens both before and after winding the vessels for a given resin system. In addition, we fabricated two groups of vessels from each epoxy system on different days to avoid possible bias in processing.

Vessel Testing

All vessels were tested by hydrobursting at a constant rate of 5.9 MPa/s, using a closed-loop pressure control system. Tables 15-17 summarize the test details of over 90 vessels made from 10 epoxy resin formulations. The fiber content of these vessels was closely

Table 15. Performance of filament wound pressure vessels made from the reference epoxy systems.

Property	Epoxy System 10			Epoxy System 11				Epoxy System 12	
Resin components	ERL 2256/Tonox 60-40			ERL 2258/ZZL 0820				Epon 826/RD-2/Tonox 60-40[a]	
Gell cycle, h/ C	2/50	16/50		16/50	2/90			4/90	
Cure cycle, h/ C	3/150	2/94 + 3/150		3/163	3/150			3/150	
Composite Vessel Data[b]									
Number of specimens[c]	4	4	4	4	4	4	4	4	4
Mass, g: fiber, W_f	30.4	31.8	31.7	32.0	30.5	32.0	31.7	32.0	30.5
composite, W_c	43.0	46.0	45.6	44.3	42.7	45.4	45.9	45.3	42.7
Fiber content, V, vol%	66.5	65.1	65.6	68.1	67.3	66.5	64.9	66.9	66.1
Burst pressure, P, MPa (CV, %)	16.2 (1.1)	19.4 (2.6)	18.1 (2.9)	15.6 (6.7)	15.9 (4.4)	17.7 (1.5)	17.8 (1.1)	17.8 (1.5)	16.5 (1.9)
Vessel Performance Factors[d]									
Fiber performance, PV/W_f, MPa m³/kg (CV, %)	0.368 (1.6)	0.399 (3.9)		0.353 (5.9)	0.379 (1.0)			0.380 (1.7)	
Composite performance, PV/W_c, MPa m³/kg (CV, %)	0.522 (1.1)	0.575 (4.5)		0.492 (6.4)	0.543 (1.4)			0.534 (2.0)	
Average calculated hoop fiber stress, MPa	1974	2286		1920	2164			2091	

[a] Pot life of this epoxy system is relatively short.

[b] Vessel volume is a constant 9.75×10^{-4} m³.

[c] Two groups of four vessels each were made from different fiber spool at different times.

[d] The ± values are the 95% confidence limits.

Table 16. Performance of filament wound pressure vessels from moderate pot life epoxy systems.

Property	Epoxy System 2		Epoxy System 3		Epoxy System 4	
Resin components	XD 7818/ERL 4206/ Tonox 60-40		XD 7818/XD 7575.02/ XD 7114/Tonox 60-40		XD 7818/XD 7575.02/ ERL-4206/Tonox 60-40	
Gell cycle, h/°C	40/60		16/60		4.5/60	
Cure cycle, h/°C	3/120		4/120		3/120	
Composite Vessel Data[a]						
Number of specimens[b]						
Mass, g: fiber, W_f	32.0	30.2	32.0	30.4	31.7	30.4
composite, W_c	44.2	42.5	43.8	42.3	43.8	42.5
Fiber content, V, vol%	68.3	67.1	69.2	68.0	68.7	67.8
Burst pressure, P, MPa (CV, %)	16.7 (5.7)	15.3 (5.5)	16.4 (0.7)	16.1 (2.6)	17.1 (1.2)	15.9 (4.6)
Vessel Performance Factors[c]						
Fiber performance, PV/W_f, MPa·m³/kg (CV, %)	0.503 (5.4)		0.508 (2.3)		0.517 (3.4)	
Composite performance, PV/W_c,	0.361 (5.4)		0.368 (1.9)		0.373 (3.7)	
Average calculated hoop fiber stress, MPa	1950		1981		2011	

[a]Vessel volume is a constant 9.75×10^{-4} m³.

[b]Two groups of four vessels each were made from different fiber spools at different times.

[c]The ± values are the 95% confidence limits.

controlled to between 64.9 and 69.3 vol%. To further minimize the effect of fiber content on the vessel performance, we also calculated the vessel performance factor based on the bare fiber weight of the vessel.

During the hydroburst tests, we monitored the vessel acoustic emission (AE) and observed two trends. First, at a fixed electronic gain, the low performing vessels showed substantially more AE than did the high performing vessels. The number of AE ring-down counts for the epoxy systems that resulted in the low performing vessels was an order of magnitude greater than the number of AE ring-down counts for the high-

Table 17. Performance of filament wound pressure vessels made from long pot life epoxy systems.

Property	Epoxy System 5		Epoxy System 6		Epoxy System 8		Epoxy System 13[d]	
Resin components	XD7818/XD 7114/ Tonox LC		XD 7818/XD 7114/ Tonox 60-40/2, 6-DAP		XD 7818/XD 7575.02/ XD 7114/Tonox 60-40/ 2,6-DAP		ERE 1359/RD2/ 2,6-DAP	
Gell cycle, h/°C	4.5/60		5/60		5/60		12/80	
Cure cycle, h/°C	3/120		4/120 + 4/155		4/120 + 4/155		2/100 + 2/125 + 4/150	
Composite Vessel Data[b]								
Number of specimens[c]	4	4	4	4	4	4	4	4
Mass, g: fiber, W_f	32.1	30.6	30.4	31.8	31.8	31.9	31.8	32.7
composite, W_c	43.9	42.1	43.0	44.9	45.2	45.2	45.8	46.0
Fiber content, V, vol%	69.3	68.8	66.6	66.7	66.2	66.5	65.3	67.4
Burst pressure, P, MPa (CV, %)	15.0 (2.7)	14.6 (3.3)	13.9 (1.7)	13.7 (2.4)	14.3 (1.0)	13.4 (2.8)	14.1 (0.8)	14.1 (2.2)
Vessel Performance Factors[d]								
Fiber performance, PV/W_f, MPa·m³/kg (CV, %)	0.46 (2.9)		0.432 (4.0)		0.424 (4.0)		0.426 (2.4)	
Composite performance, PV/W, MPa·m³/kg (CV, %)	0.336 (3.2)		0.305 (3.7)		0.298 (3.7)		0.299 (1.5)	
Average calculated hoop fiber stress, MPa	1804		1682		1688		1719	

[a]New epoxy system developed by the U.S. Navy and tested at their suggestion.

[b]Vessel volume is a constant 9.75×10^{-4} m³.

[c]Two groups of four vessels each were made from different spools of fiber at different times.

[d]The ± values are the 95% confidence limits.

Fig. 23. Typical pressure vessel failures: from left to right, vessels made with epoxy systems 1, 4, and 7.

performing epoxy systems. Second, the peak amplitude of many AE signals generated in the low performing vessels was three times higher than the AE signals generated in the high performing vessels.

The typical hoop failures experienced by the pressure vessels are shown in Fig. 23. A key observation with respect to the failed vessels is that in the low performance epoxy systems, failure was localized and involved only a relatively small portion of the hoop wraps. Conversely, in the high performing epoxy systems, vessels failures involved almost all of the hoop wraps.

Limited data on composite shear properties were obtained for several composites. Table 18 summarizes these results.

Discussion

Fiber content in wet wound composites is difficult to control. There is some qualitative evidence for S-glass/epoxy and high-modulus organic/epoxy composites indicating that fiber strength is definitely affected by fiber content. Therefore, this factor must be taken into consideration when comparing epoxy performance in composites. In this study, we simply controlled the volumetric fiber content to a practical range, both for the strand specimens and for the pressure vessels.

As shown in Table 14, when the fiber content of the strand specimens made from five spools of Kevlar 49 fiber and nine epoxies was held between 61 and 65 vol%, the average fiber strength varied only by about 10%. This is not sufficient evidence to allow us to conclude that the effect of the epoxy formulations is statistically significant. However, our previous study using only one epoxy did show that Kevlar 49 had a 6% CV in strength. In addition, our unpublished data on S-glass strands impregnated with more than 10 typical epoxies led to the same conclusion—the epoxy has no significant effect on strand strength.

Conclusions

From the above studies of various epoxy resin systems and the performance of composite pressure vessels using these resins, we draw the following conclusions:

- In the absence of vessel performance data, we propose that resin selection criteria be based, in order, on (1) processing considerations, (2) neat resin properties, and (3) commercial availability of the resin components.

Table 18. In-plane and interlaminar shear properties of Kevlar 49 fiber in several epoxies.

Property	Moderate pot life systems		Long pot life systems		Reference systems	
Resin system No.	2	4	5	8	10	12
Gell cycle, h/°C	2.5/80	4.5/60	5/60	5/80	16/50	3/60
Cure cycle, h/°C	2/160	4/120	3/120	3/120	2/120	2/120
In-Plane Shear Properties (±45-deg Laminate)						
Number of specimens	3	3	5	5	3	4
Strength at yield, MPa	20.2	21.6	32.4	41.4	20.9	22.8
Shear modulus to 0.005 strain, GPa (CV, %)	1827 (2.1)	1730 (2.9)	1903 (4.2)	1889 (1.7)	1685 (2.5)	1565 (3.5)
Interlaminar Shear Properties (ASTM-D-2344, Short Beam)						
Number of specimens	12	15	12	12	15	12
Strength, MPa (CV, %)	34.6 (4.5)	30.0 (5.1)	38.4 (3.5)	45.9 (3.4)	29.3 (3.9)	36.8 (3.9)

- In a normal wet winding process where an extra-long pot life is not very critical, the top candidate epoxy system to replace the ERL-2256 system is plain or rubber-modified DGEBF resin diluted with VCHDO and cured with Tonox 60-40 (formulations 2 and 4 in Table 11).
- In a winding process where an extra-long pot life is required, plain or rubber-modified DGEBF resin, diluted with the diglycidyl ether of neopentylglycol offers good elongation (and perhaps good flexibility) when cured with either 2,6-DAP or Tonox 60-40 (formulations 5, 6, and 8 in Table 12). From a cost and processing standpoint, we consider Tonox LC to be a better curing agent than 2,6-DAP.
- Within the narrow range of fiber content studied, the effect of these selected epoxy systems on the fiber strength of unidirectional, epoxy-impregnated strands is insignificant. However, for a pressure vessel under multiaxial loading, the effect of the epoxy system on vessel performance is indeed noticeable (25% change in mean burst pressure).
- The epoxy system containing 5% CTBN, rubber-modified DGEBF, diluted with VCHDO and cured with mixed aromatic amines (formulation 4, Table 11), appears to be the best resin matrix for filament winding to replace the epoxy systems no longer commercially available.

References

13. T. T. Chiao, E. S. Jessop, and L. Penn, "Screening of Epoxy Systems for High Performance Filament Winding Applications," presented at *7th Natl. SAMPE Tech. Conf.*, October 14-16, 1975, Albuquerque, NM.
14. T. T. Chiao and L. P. Althouse, "Characterization of an Epoxy System for Filament Winding," in *Proc. 4th Natl. SAMPE Tech. Conf.*, October 17-19, 1974, Palo Alto, CA.
15. W. D. Bascon, "Adhesive Fracture Behavior of Elastomer-Modified Epoxy Resins," in *Proc. 30th Reinforced Plastics/Composites Institute, S.P.I. Section 22-D*, February 4-7, 1975, Washington, D.C.
16. T. T. Chiao, E. S. Jessop, and H. A. Newey, "An Epoxy System for Filament Winding," *SAMPE Quart.* 6(1) (1974).
17. T. T. Chiao, A. D. Cummins, and R. L. Moore, "Fabrication and Testing of Epoxide Resin Tensile Specimens," *Composites* 3(10) (January/February 1972).
18. T. T. Chiao, E. S. Jessop, and M. A. Hamstad, "Performance of Filament Wound Vessels from an Organic Fiber in Several Epoxy Matrices," in *Proc. 7th Natl. SAMPE Tech. Conf.*, October 14-16, 1975, Albuquerque, NM.

PART III. KEVLAR 49/EPOXY PRESSURE VESSELS WITH POLYMER LINERS

Polymer Systems for Vessel Liners[19]

Evaluation of Liner Materials

To overcome the problem of metal liner fatigue, we initiated a program to develop a flexible polymeric liner with a low permeability to nitrogen gas and a high fatigue life. Published permeability coefficients indicate that two polymeric materials have especially low permeability to nitrogen gas—Saran (polyvinylidene chloride), and Parylene C [poly(monochloro-paraxylylene)]. Table 19 presents the nitrogen gas permeabilities of these two materials as reported by the manufacturers.

Three types of laminated flat specimens were prepared for the standard permeability test: 0.38-mm-thick butyl rubber sheet, the same butyl rubber sheet coated on one side with a 0.064-mm-thick layer of Parylene C, and the same butyl rubber sheet coated on one side with a 0.27-mm-thick layer of Saran latex XD 7151.00. The Parylene C coating was applied by chemical vapor deposition (CVD) and the Saran latex was applied by painting or spraying. For the CVD coating, the rubber sheet was placed in a room-temperature vacuum chamber. The chamber was evacuated and the Parylene C vapor was drawn through by the vacuum pump. It took several hours to apply the thin coating. The Saran latex was painted on the flat laminate specimens in several layers. After each layer was applied, the Saran was dried at room temperature.

We determined the nitrogen gas permeabilities of the three different types of laminated films according to ASTM D-1434-66, Method M. In each case, the butyl rubber was placed opposite the nitrogen gas source. The permeability coefficients of the Saran latex and Parylene C films were calculated assuming that classical gas permeation theory applies and assuming that there is no interaction between the diffusing gas and the laminations (see Table 19). These results indicate, as the published data suggest, that the Saran-coated butyl rubber makes the better nitrogen barrier, being approximately two orders of magnitude less permeable to nitrogen than butyl rubber alone and about one order of magnitude less permeable than Parylene C-coated butyl rubber. On the basis of these results, we began tests of actual pressure vessels lined with these materials.

Polymer-Lined Pressure Vessels

Cylindrical pressure vessels, 10.3 cm in diameter with aluminum fittings and 0.050-cm-thick chlorobutyl rubber liners coated with Saran and Parylene C, were filament wound with Kevlar 49 fiber in an epoxy matrix (see Fig. 24). Details on such filament wound vessels have been published previously.[20, 21] During winding, the liners were supported by water-soluble salt mandrels. Four vessels were prepared with the same winding pattern. One vessel had both Saran latex and Parylene C coatings, another vessel had only a Saran coating, and two vessels had only Parylene C coatings. The vessels were first gelled for 16 h at room temperature and then cured for 3 h at 90°C. Table 20 summarizes

Table 19. Nitrogen gas permeability of various polymer liner materials.

Material	Permeability constant, 10^{12} cm³ STP·cm/cm²·cm Hg		
	Published or supplier's value	Experimental value[a,b]	Calculated from experimental value[c]
Saran latex (XD 7151.00)	0.018 to 0.042	—	0.15
Parylene C	0.6	—	0.60
Butyl rubber	32	26, 10[d]	—
Butyl rubber coated with Parylene C	—	3.7	—
Butyl rubber coated with Saran latex	—	0.37[e]	—

[a] Average of two runs unless otherwise noted.

[b] The limitation of the experimental equipment is reached at 10^{-1}.

[c] Assumes that classical gas permeation theory applies and that there is no interaction between the diffusing gas and the laminations.

[d] Flat specimen of liner material.

[e] Single test.

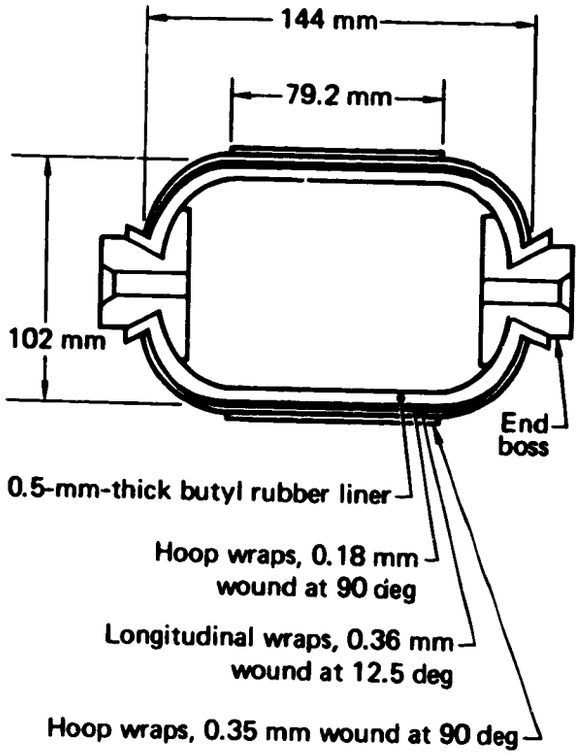

Fig. 24. Dimensions of the 10.2-cm-diameter pressure vessel (volume = 950 ± 8 cm³); thicknesses of coating are not shown.

the winding patterns and other pertinent fabrication data; the detailed construction of each of these vessels is shown in Fig. 25.

In the permeation tests, the vessels were pressurized with nitrogen in a temperature-controlled (21 ± 3°C) test chamber. The piping and valves used in the pressurization system were all leak-checked with helium gas before testing. The four vessels were pressurized to about 11.7 MPa (about 65% of the expected burst pressure based on previous vessels of the same design but without the coatings). The vessels were then valved off for about 4 h. Each vessel was topped off to about 11.7 MPa and valved off for the remainder of the test. Four calibrated, bourdon-type pressure gages on the vessel side of the isolation valves were used to obtain periodic pressure readings. Figures 26 through 29 show the pressure in the vessels as a function of time, both for the 4-h stabilization period and for the remainder of the test. The pressure is shown in terms of percentage of the pressure at valve-off. The large day-to-day pressure fluctuations shown in the figures are the result of outside air temperature effects (see Fig. 26) on the pressure gages. Because fluctuations in the temperature of the vessels themselves were rather small and on both sides of the average value of 21°C, no attempt was made to correct for temperature changes.

Discussion

Using classical permeation theory and the permeability coefficients determined from the flat laminate specimens, we calculated the approximate nitrogen pressure loss through the pressure vessel walls for the 3-mo period. We assumed that the fiber/epoxy composite is porous and that the wall thicknesses of the butyl rubber and coatings do not change with pressurization. In Table 21, we present the results of these calculations for the four polymer-lined vessels, for a vessel with only a butyl rubber liner, and for a vessel in which we assumed that only the inner Parylene C coating is effective. These calculations neglect the small increase in surface area that occurs with pressurization as well as the small differences between the surface area of the coatings on the inside of the liner and those on the outside of the composite. To accommodate these factors, an average surface area of 460 cm² was used for all calculations. For comparison, the actual percentages of pressure lost are also recorded in Table 21.

It appears that vessel 3 had some type of leak, either a pinhole or a pressure fitting leak. A retest of this vessel with new fittings indicated that the leakage was caused by a faulty pressure fitting. The actual pressure loss rates in the other three vessels were all about the same. After the first few days, these loss rates were very close to the theoretical prediction for the inner Parylene C coating alone. Theoretically, vessel 4 (Saran-coated) should have a substantially lower loss rate (sevenfold) than vessels 1 and 2. We conclude that the Saran coating on vessel 4 is not as effective as the tests of the flat laminate specimens led us to expect. The greater than expected permeation through the Saran coating may have resulted from straining of the coating during pressurization.

Some experimental and theoretical work was undertaken to explore the possibility of strain-enhanced permeability. In general, the experimental work revealed an increase in permeability, usually less than an order of magnitude, for strains of 5% or more. Unfortunately, this effect in Saran has not been specifically studied. Even if such studies had been made, it is unlikely that the strain states present in the pressurized vessels could be determined. It is well known that the two principal strains in the plane of the vessel walls are on the order of 1% tensile strain[20, 21]; the compressive strain through the wall thickness is not known.

The most important result of this permeability study is the demonstration of a low nitrogen-pressure loss rate in a very lightweight pressure vessel. The performance factor for this type of pressure vessel, excluding the boss mass, is approximately 0.200 MPa·m³/kg. This is in comparison to a maximum performance factor of about 0.170 MPa·m³/kg for a

Table 20. Fabrication data for the 10.2-cm-diameter, cyclindrical Kevlar 49/epoxy[a] pressure vessels.

Property	Vessel No. 1	2	3	4
Vessel Data				
Volume, cm^3	949	949	949	949
Expected burst pressure, MPa	17.9	17.9	17.9	17.9
Liner mass,[b] g	38	38	52	59
Expected performance factor, MPa·m^3/kg: composite + liner	0.204	0.204	0.174	0.164
composite	0.376	0.375	0.375	0.366
Composite Data				
Composite mass, g	45.2	45.3	45.3	46.4
Fiber mass, g	32.4	32.7	34.9	34.5
Fiber content, vol%	67.7	68.2	73.0	70.4
Winding Data[c]				
Longitudinal angle, deg		13		
Hoop/longitudinal fiber ratio		1.7		
Winding pattern		36-band, closed		
Layers (interspersing)[d]: hoop		6(2 + 4)		
longitudinal		4(none)		
Total winding circuits: hoop		858		
longitudinal		1080		
Extra reinforcement at the equator, circuits		60		

[a]Epoxy system is DER 332/T-403 (100/39 parts by weight), gelled for 16 h at 21 C and cured for 3 h at 90 C.

[b]Calculated from known density.

[c]Winding data are the same for all four vessels.

[d]Sequence is 2 hoop layers, 4 longitudinal layers, then 4 hoop layers.

homogeneous metal pressure vessel. Thus, this composite pressure vessel is comparable in burst performance to an all-metal vessel and experiences no significant pressure loss due to leakage for more than 3 mo.

Fatigue Life of Polymer-Lined Kevlar 49/Epoxy Pressure Vessels[22]

Basis for Study

Fatigue lives for complex structures under complex states of stress cannot yet be predicted from laboratory data for simple specimens. Therefore, we have studied a typical filament wound fiber/epoxy structure under fatigue loading, using enough specimens to ensure statistical confidence in the results.

We chose a 10.2-cm-diameter, filament wound pressure vessel as the test structure. We studied the burst pressure and fatigue life distribution of 150 vessels. The stress rupture life also was determined for a limited number of these vessels.

Materials and Specimens

We chose Kevlar 49 as the fiber and used the ERL 2258/ZZL 0820 epoxy system for the matrix. The epoxy system was gelled at 60°C for 16 h and cured at 163°C for 2 h. In earlier studies, we had characterized the fiber, epoxy, and composite. The typical single-end fiber (nominally 380 denier with 280 filaments) had no finish, but had a twist of about 3 turn/m. The fiber failure stress of a typical epoxy-impregnated strand was 3480 MPa.

The design of the 10.2-cm-diameter, butyl-rubber-lined, cylindrical pressure vessel used for these tests is shown in Fig. 30. The vessels were prepared according to the following procedure. Before winding, each spool of fiber was dried in a vacuum oven for 24 h at 82°C and at a pressure <700 Pa. Over a period of about 5 wk, 150 vessels were wound with the same pattern on a numerically controlled winding machine. The fiber strand was epoxy-impregnated inside a vacuum chamber held at approximately 650 Pa. We used a constant 4.5-N winding tension. Other details on the 10.2-cm-diameter vessel are given in Table 22.

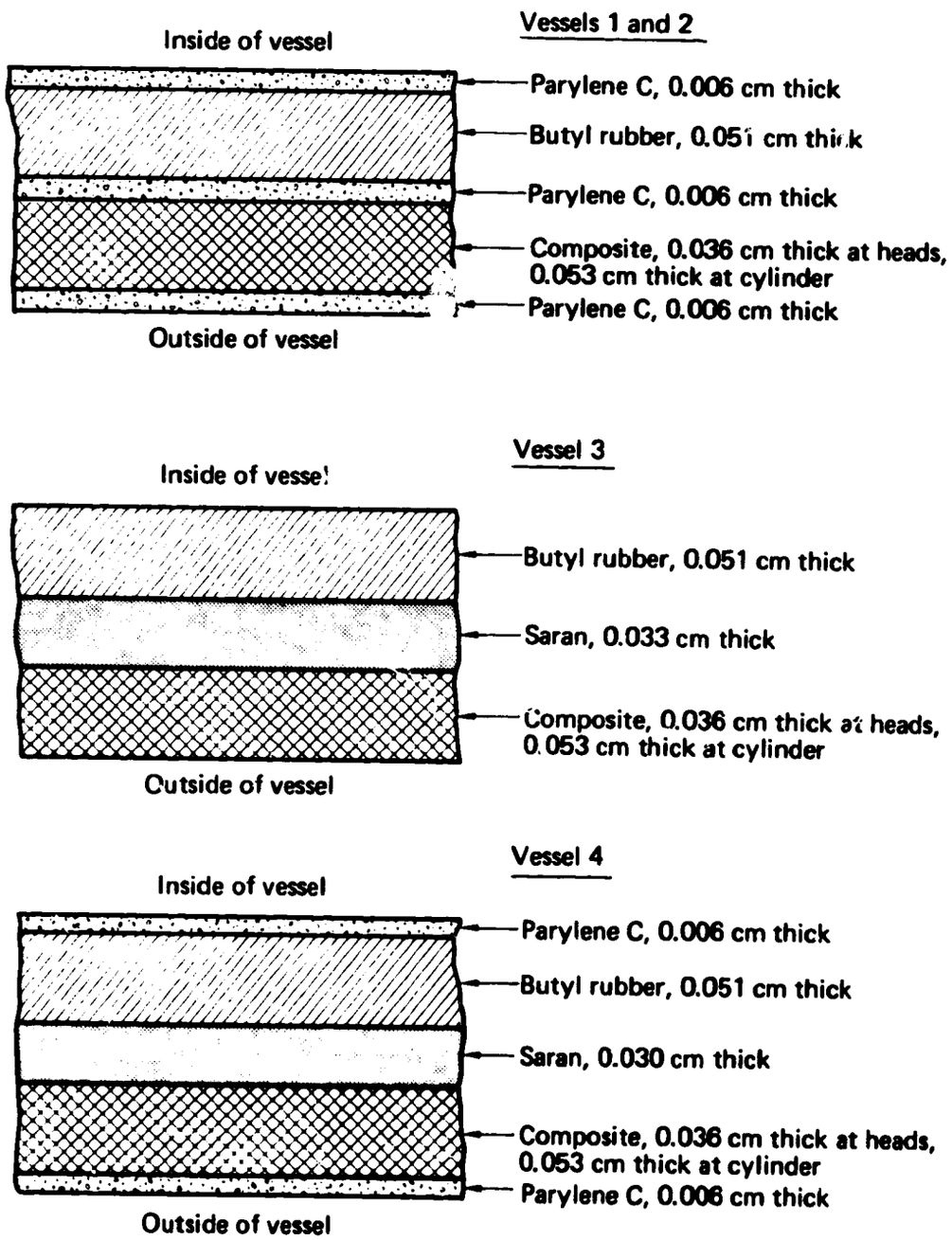

Fig. 25. Wall cross sections of four vessels tested showing the dimensions of the various coatings used.

Table 21. Nitrogen pressure loss over 3 mo for 10.2-cm-diameter, polymer-lined, filament wound Kevlar 49/epoxy pressure vessels.

Coating	Vessel No.	Calculated loss, %	Experimental loss, %	Calculated loss,* %
3 layers of Parylene C	1	0.38	1.8	1.2
3 layers of Parylene C	2	0.38	2.4	1.2
1 layer of Saran	3	0.055	100	100
1 layer of Saran + 2 layers of Parylene C	4	0.055	1	1.2
No coating, butyl rubber only	control	6.2	—	100

*Assuming that only the inside Parylene C coating is effective.

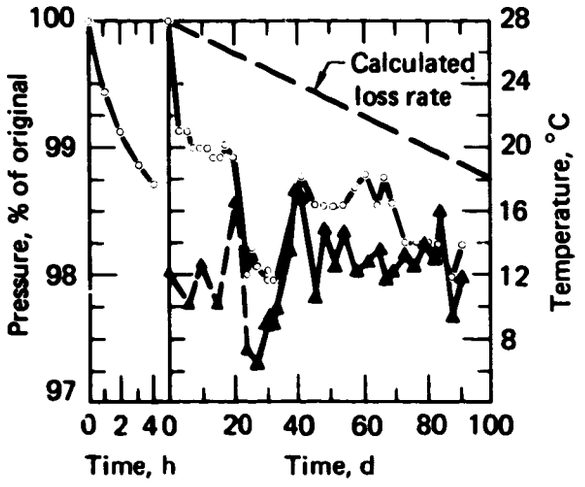

Fig. 26. Percentage of original nitrogen pressure vs time and ambient air temperature vs time for vessel 1: ○ = gage pressure, ▽ = temperature as read at thermometer near Heise gage, ▲ = temperature as estimated from outside air temperature 2 mi away.

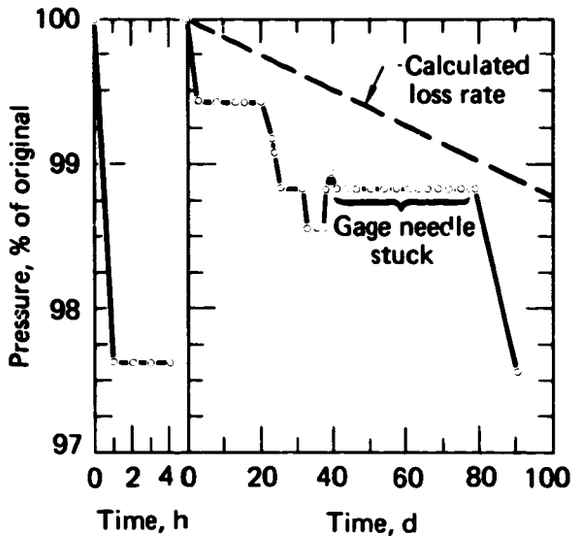

Fig. 27. Percentage of original nitrogen pressure vs time for vessel 2.

The design of the winding pattern predisposed the vessels to fail in the hoop wraps. We decided that control of the failure location would allow better interpretation of the results. For this reason, the few vessels that failed at other locations were not included in the statistical analyses.

Experimental Conditions

The vessels were stored in an air-conditioned laboratory environment until testing. Random groups of the vessels were pressurized internally with water-soluble oil to determine the following distributions: burst pressure for monotonic loading to failure, cyclic life to failure under sinusoidal pressure cycling, cyclic life to failure under rectangular pressure cycling, and stress-rupture life to failure. A closed-loop feedback control system regulated all pressurization tests. The burst tests were conducted at a constant pressurization rate of 115 kPa/s to failure. An electronic (strain-gaged diaphram) pressure transducer, located about 0.6 m from the pressure vessel, measured the failure pressure.

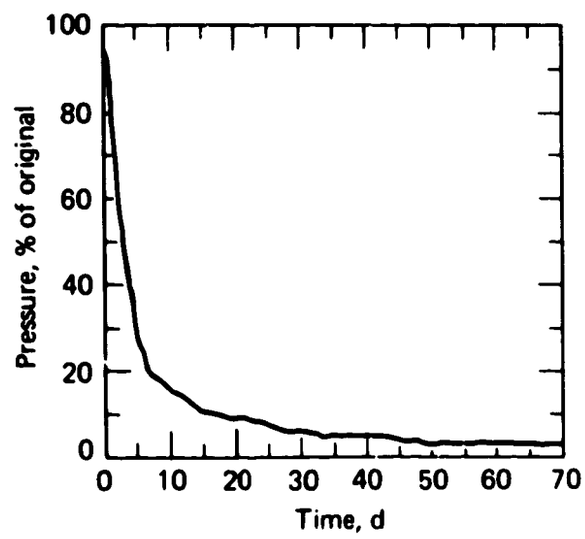

Fig. 28. Percentage of original nitrogen pressure vs time for vessel 3.

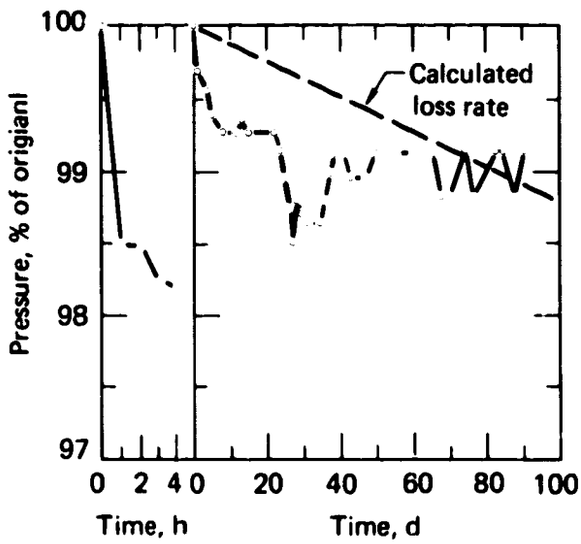

Fig. 29. Percentage of original nitrogen pressure vs time for vessel 4.

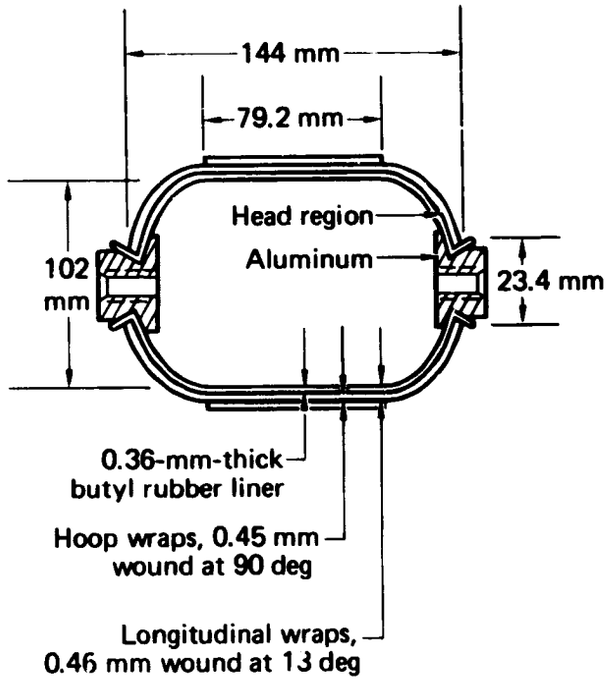

Fig. 30. Design of the 10.2-cm-diameter pressure vessel (volume = 950 ± 8 cm³) used for fatigue testing.

Pressure was applied to one group of 25 vessels in sinusoidal cycling at a rate of 1 Hz. The upper and lower pressures were 91 and 4% of the mean failure pressure determined in the burst tests. We used an amplitude detection instrument combined with an oscilloscope to control the upper pressure to within ±0.5%. For these tests, the pressure transducer was located just a few centimeters from the pressure vessel. We compared measurements from pressure transducers on either side of one pressure vessel to confirm that rate effects were not causing the pressure in the vessel to differ from the pressure at the transducer. To verify that no significant heating effects were caused by the test rate, we instrumented one vessel with a thermocouple. At the test rate of 1 Hz, the temperature increased less than 5°C.

Pressure was applied to another group of vessels in rectangular cycling at a rate of 0.33 Hz. As with the sinusoidal cycles, the upper and lower pressures were 91±0.5 and 4% of the mean burst pressure. The actual pressure pulses experienced by the pressure vessels were not perfectly rectangular. Oscilloscope photographs of the pressure pulse experienced by a pressure transducer a few centimeters from a vessel revealed that the rise time of the pressure pulse was about 0.14 s and the peak pressure per cycle lasted about 1.36 s. A trace of such an oscilloscope photograph of this rectangular pressure pulse is shown in Fig. 31. Again, comparison of pressure readings from transducers on opposite sides of a vessel assured us that the pressure experienced by the vessel was the same as that at the transducers.

The stress rupture tests were performed at a pressure of 91±0.5% of the mean burst pressure. Vessels were first loaded to 80% of the mean burst pressure;

Table 22. Characteristics of 10.2-cm-diameter, cylindrical Kevlar 49/epoxy[a] pressure vessels.

Property	Value
Winding Data	
Longitudinal angle, deg	13
Winding pattern	36-band, closed
Layers (interspersing): hoop	6 (none)
longitudinal	4 (none), 8.9-mm bandwidth
Total winding circuits: hoop	810
longitudinal	1080
Extra reinforcement	none
Composite Data	
Wall thickness, mm: hoop	0.45
longitudinal	0.46
Mass, g (CV, %)[b]: composite	42.4 (2.3)
fiber	30.4 (2.3)
total vessel[c]	162
Fiber content, vol% (CV, %)	67.8 (2.8)

[a] Epoxy system is ERL 2258/ZZL 0820 (100/30 parts by weight), gelled for 16 h at 60°C and cured for 3 h at 163°C.

[b] Average of 25 vessels.

[c] Including aluminum fittings and liner.

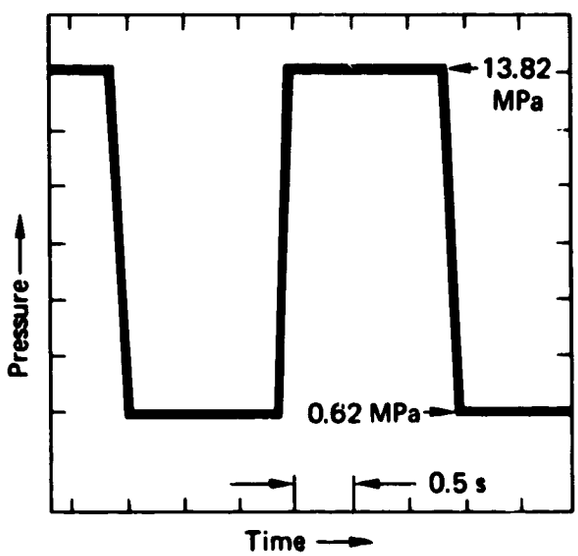

Fig. 31. Actual shape of the nominally rectangular pressure pulse.

then the pressure was increased at a constant rate, reaching the 91% level in less than 5 s. Oscilloscope photographs of the pressure as applied to the vessels ensured that there was no pressure overshoot. A continuous plot of vessel pressure vs time verified that the pressure remained within the designated limits throughout the test.

All the pressure vessels tested in fatigue or stress rupture were first proof tested to 80% of the mean failure pressure determined during the burst tests. The test pressurization rate was 58 kPa/s. The pressure was held at the 80% load level for 30 s, after which the vessel was rapidly depressurized.

Results

The burst pressures for 25 vessels are shown in Table 23. To facilitate later discussion, we have ordered the burst pressures from the lowest to the highest. The mean burst pressure was 15.2 MPa with a CV of 4.5%. All 25 vessels failed in the hoop wraps. Photographs of a vessel before failure and of two vessels after failure are given in Fig. 32. During the burst tests, one vessel failed in the head region; this vessel was not included in the statistical analysis for the reasons discussed above. Strain was plotted vs the internal pressure data obtained from strain gages bonded in the axial and hoop directions (see Fig. 33).

The number of sinusoidal cycles to vessel failure for another 25 vessels are recorded in Table 22. We have ranked the cyclic lifetimes from the lowest to the highest. All of these vessels had failures originating in the hoop wraps during cycling, except for one vessel that failed during the first cycle and was not included in the statistical analysis.

Table 22 also records the number of rectangular cycles to vessel failure for a third set of 25 vessels. In addition to ranking the lifetimes for these vessels, we have recorded the time spent at peak pressure during the test. This value was obtained by multiplying the typical time at the peak stress per cycle by the number

Table 23. Results of burst tests and fatigue tests, and computed peak stress levels of 10.2-cm-diameter Kevlar 49/epoxy pressure vessels.

Burst pressure,[a] MPa	Sinusoidal Pressure Cycle	Rectangular Pressure Cycle		
	Cyclic life, 10^3 cycles	Cyclic life, 10^3 cycles	Total time at peak stress, h	Assumed actual peak stress level, % of burst pressure
13.69	0.001	0.001	0.000 0	101.1
13.93	0.029	0.012	0.004 7	99.3
14.41	0.635	0.031	0.012 0	96.0
14.44	1.030	0.050	0.019 0	95.8
14.55	3.440	0.083	0.032 0	95.1
14.75	4.230	0.088	0.034 0	93.7
14.79	11.800	0.242	0.094 0	93.5
14.89	12.100	0.393	0.150 0	92.9
14.96	12.600	2.740	1.100 0	92.4
15.00	14.300	3.680	1.400 0	92.2
15.10	18.800	4.030	1.600 0	91.6
15.24	22.300	4.690	1.800 0	90.8
15.27	24.500	7.060	2.800 0	90.6
15.34	27.100	7.140	2.800 0	90.2
15.38	35.600	7.210	2.800 0	90.0
15.38	88.700	7.640	3.000 0	90.0
15.38	95.200	12.000	4.700 0	90.0
15.51	104.000	14.500	5.600 0	89.2
15.62	129.000	14.700	5.700 0	88.6
15.72	132.000	19.400	7.600 0	88.0
15.72	144.000	22.200	8.600 0	88.0
16.00	176.000	26.400	10.000 0	86.5
16.10	193.000	45.000	18.000 0	85.9
16.34	200.000	45.100	18.000 0	84.6
16.38	430.000	54.300	21.000 0	84.5

[a]All are hoop failures, (one other vessel, not included in this list, failed on the dome at 12.27 MPa).

Fig. 32. Photograph of two typical hoop failed vessels (a, b) and a typical unfailed pressure vessel (c).

of cycles to failure. Again, all 25 vessels had failures originating in the hoop wraps. Two additional vessels failed in the heads, one after four cycles and one after 134 cycles; these vessels were not included in the statistical analysis of the set of vessels.

The times to failure or test termination in the limited stress rupture tests are 154 and 235 h to failure, and 557, 543, and 531 h without failure (test termination). The vessels that failed, failed in the hoop wraps.

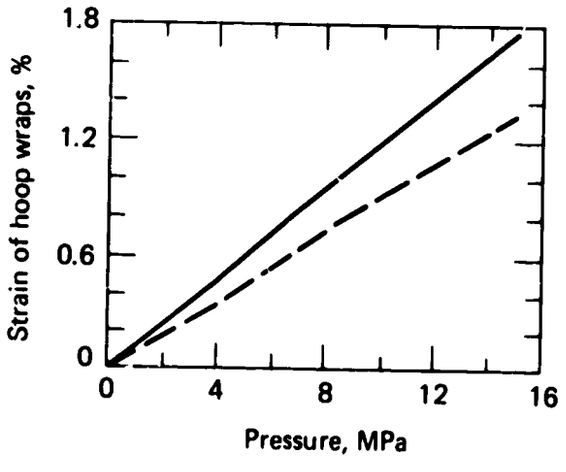

Fig. 33. Axial (dashed curve) and hoop (solid curve) strain vs internal pressure during burst testing: solid curve denotes hoop strain, dashed curve denotes axial strain.

Discussion

The results in Table 23 reveal that vessel fatigue life at the 91% load level depends on the wave shape of the pressure pulse. The mean life for vessels tested under the sinusoidal wave was 75 000 cycles, with a standard deviation of 100 000 cycles. The mean life for vessels tested under the rectangular wave was only 12 000 cycles, with a standard deviation of 15 000 cycles. Because of the large spread in the fatigue data, the mean lifetime values are only relative. We use these lifetimes only to conclude that vessels last approximately six times longer when pressure is applied in the sinusoidal wave shape than when pressure is applied in the rectangular wave shape. Thus, we believe that the time at peak pressure is a significant factor in determining the fatigue life of these composite pressure vessels at high fiber stress levels.

At first, we believed that pressure vessel fatigue life might be governed by the stress rupture properties of the vessels. If this were so, the total time at the peak pressure in the rectangular pulse tests would correspond to the stress rupture life. However, our stress rupture data indicate that this conclusion is not valid. The vessels tested in stress rupture lasted much longer than is predicted by summing the total time at peak pressure for the rectangular wave fatigue tests (minimum 0 h, maximum 21 h, mean, 4.5 h).

Hence, we conclude that the fatigue life of the vessels at the 91% load level depends on both the number of stress cycles and the time at peak pressure during

each cycle. Because the relative influence of these two factors is unknown, it is not clear whether the data presented here can be extended to other wave shapes and cyclic test rates. Furthermore, because the cyclic lifetimes vary fifty- to sixty-fold, statistically valid experimental determination of design data for different cyclic conditions will require a large number of specimens.

We have tested pressure vessels only at one high stress level, 91%, and our data do not predict the cyclic lifetime at lower stress levels. We did not test vessels at the lower pressure levels (e.g., 50%) which would be closer to actual applications for such pressure vessels because preliminary tests at the 80% load level indicated extremely long lifetimes. Thus, testing 25 specimens at such levels would be too time consuming and too expensive.

To obtain some idea of how the fatigue life might vary as a function of stress level, we made two assumptions. First, we assumed that the distribution of burst pressures for the 25 vessels that were burst tested exactly represent the distribution of expected burst pressures for each additional set of 25 vessels taken from the population of 150 vessels. Second, we assumed that there was a one-to-one correspondence between the expected burst pressure and the vessel fatigue life; i.e., the vessel with the highest expected burst pressure was the one with the greatest fatigue life. On the basis of these two assumptions, the actual upper stress level expected during the fatigue testing was calculated (see Table 22).

Using these expected upper stress levels, we plotted the cyclic lifetimes for both sinusoidal and rectangular pressure cycling (Fig. 34). If the assumptions that led to this figure are correct, extrapolation of the data in this figure indicates a very long vessel fatigue life at an upper stress level of 50%.

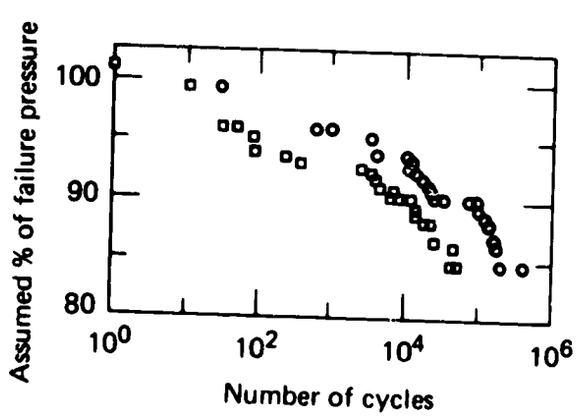

Fig. 34. Fatigue life at assumed peak cyclic stress levels for 10.2-cm-diameter pressure vessels: ○ denotes failure of vessels under sinusoidal cycling, □ denotes failure of vessels under rectangular cycling. Vessels that failed at less than one cycle are plotted at one cycle.

Almost all the failures of the filament wound vessels originated in the hoop wraps: the hoop wraps are somewhat like a unidirectional composite tube that is being stressed biaxially. Because the macroscopic composite strain is elastic, we can estimate from Fig. 33 that the axial strain change (perpendicular to the fiber direction) was about 1% per cycle, and that the hoop strain change was about 1.5% per cycle. However, the strain in the axial direction is deceiving because the hoop composite already has cracks parallel to the fibers. For this reason, these results could not be duplicated by biaxially testing a simple unidirectional composite tube for the same strain ranges.

The results presented here should not be extended to other load levels or to other strain rates without extensive testing of cylindical pressure vessels where failures originate outside of the relatively uniformly stressed hoop wraps. The composite vessel is not a unidirectional structure in the head region and the stress state here differs from that in the hoop wraps.

Full-Scale Kevlar 49/Epoxy Pressure Vessels with Polymer Liners[23, 24]

Vessel Design

In the previous experiments,[24] we designed and tested four 10.2-cm-diameter pressure vessels lined with alternating layers of rubber and polymer (Figs. 24 and 25). On the basis of that design, we fabricated two proportionately larger vessels, one 20.3 cm in diameter (approximately twice the size of the 10.2-cm-diameter vessel) and one 38 cm in diameter (a full-size replica of the one used in the NASA tests).

Twenty-one 20.3-cm-diameter vessels were wound, the first three with 380-denier Kevlar 49 fiber and the rest with 1420-denier fiber. Both denier fibers had comparable tensile strengths so that the change did not degrade vessel performance. (Ten tensile tests on the 1420-denier fiber/epoxy strands gave an average fiber stress of 3360 MPa vs 3510 MPa for the 380-denier fiber strands.) In addition, by switching to the larger denier fiber, we reduced fabrication time to less than one 8-h shift per vessel. After winding and testing eight vessels, the winding pattern was fixed (Table 24). Vessels intended for permeation studies were wound on Saran-coated mandrels.

Five 38-cm-diameter vessels were wound, four with a special 4-end, 4560-denier roving (Fig. 35); the winding time was approximately 10 h per vessel. The fifth vessel was wound with 1420-denier fiber in 22 h. Once again, fiber choice was based on the length of winding time (10 h vs 22 h) and on tensile

Table 24. Performance and winding pattern of the rubber-lined, 20.3-cm-diameter Kevlar 49/epoxy pressure vessels (0.5-mm-thick liner, 23°C test temperature).

Property	Vessel No.						
	K1	K2	K3	K4	K5	K6	K7
Vessel Data[a]							
Burst pressure, MPa	28.10	29.65	Leaked	28.13	29.72	26.34	24.82
Failure location[b]	K + H	K + H	—	H	H	K	H
Fiber performance, MPa·m³/kg	0.443	0.436	—	0.421	0.414	0.359	0.384
Composite performance, MPa·m³/kg	0.330	0.333	—	0.333	0.313	0.375	0.271
Composite Data							
Composite mass, kg	0.8043	0.8404	0.8533	0.7990	0.8376	0.9309	0.8653
Fiber mass, kg	0.5993	0.6425	0.6390	0.6324	0.6336	0.6944	0.6110
Fiber content, vol%	70.5	72.2	71.9	75.9	71.3	70.5	66.5
Winding Data[c]							
Winding tension	17.8	17.8	17.8	17.8	17.8	17.8	17.8
Longitudinal angle, deg	7	7	7	7	7	7	7
Hoop/longitudinal fiber ratio	1.7	1.6	1.6	1.5	1.5	1.57	1.55
Layers (interspersing): hoop	20(8 + 12)	26(8 + 18)	28(8 + 18)	28(8 + 20)	16(4 + 12)	16(4 + 12)	16(4 + 12)
longitudinal	14(none)	16(none)	16(none)	16(none)	8(none)	8(none)	8(none)
Total winding circuits: hoop	8952	9341	6354	6354	2464	2624	2600
longitudinal	8316	9216	9216	9216	2448	2592	2592
Extra reinforcement at the equator, circuits	Hoop 80 + Helical 95	Hoop 130	Hoop 126	Hoop 30	Hoop 30	Hoop 35	Hoop 40
Epoxy Resin Data[d]							
Gell cycle, h/°C	16/21	58/21	18/21	18/21	18/21	18/21	18/100
Cure cycle, h/°C	3/80	3/80	3/80	3/80	2/21	2/121	3/176

[a] Vessel volume a constant 9.453×10^{-4} m³.

[b] H = hoop failure, F = fitting failure, K = knuckle failure.

[c] A 36-band, closed winding pattern was used for all vessels.

[d] The resin system XD 7818/T-403 (100/49 parts by weight) was used for all vessels.

strength. (Eight elongated NOL rings were wound with 1420-denier fiber and eight with 4560-denier roving: the 1420-denier fiber had an average failure stress of 2740 MPa and the 4560-denier roving had an average failure stress of 2590 MPa.) Table 25 lists the final winding pattern. Table 26 summarizes the pattern design for the three vessel sizes (see Fig. 24), and Fig. 36 gives a physical comparison of the three sizes of vessels.

Vessel Tests

To determine the effects of scaling up the vessel design, we fabricated 20.3-cm-diameter, polymer-lined pressure vessels and subjected them to burst, permeation, and fatigue tests. When we subjected 10 of the 21 vessels wound to burst tests (see Tables 24, 27, and 28), several problems were encountered. First, there was significant liner leakage with four of the vessels. Second, the average composite performance was low, partly because end failures were the primary mode of failure. The axial and hoop strain measurements for one of the vessels are plotted in Fig. 37. A photograph of a failed vessel where hoop failure was the primary failure mode is given in Fig. 38.

Because of the obvious failure of the Parylene C and Saran coatings, we made several changes in the manufacture and repair procedures. This liner leakage problem, the various attempted solutions, and the results obtained are discussed in the following section.

We subjected four of the 20.3-cm-diameter vessels to the nitrogen gas permeation test. All vessels leaked to zero pressure in just a few days. We then fatigue cycled four other vessels and found significant liner leakage after less than 40 cycles. Suspecting a lack of total cure of the butyl rubber liner, we post-cured the remaining three vessels (originally scheduled for testing by NASA) at 121°C for 3 h. One of these vessels was burst tested and the other two were cycled to 70% of the expected burst pressure. A burst pressure

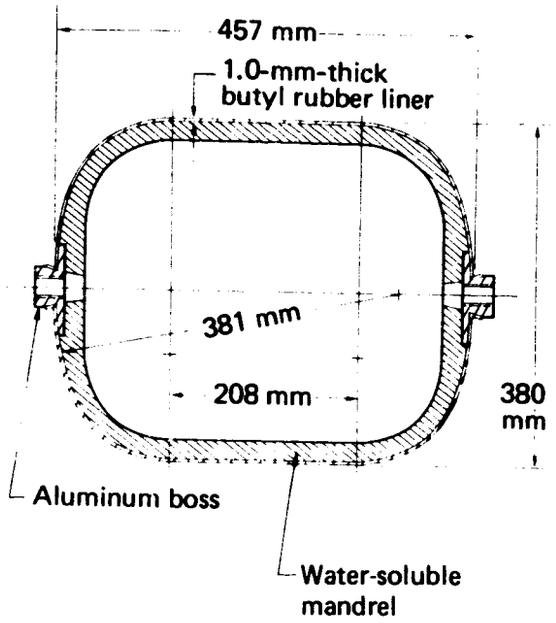

Fig. 35. Mandrel design for the 38-cm-diameter pressure vessels.

of 27.6 MPa was obtained with no sign of liner leakage. The two cycled vessels survived 100 cycles and 23 cycles; failure was found to be caused by leakage through the liner. The liner leakage problem was not fully understood at this point in the experiment.

We also fabricated and burst tested four 38-cm-diameter vessels. The first vessel could not be burst because the rubber liner leaked (the liner was of poor quality). All subsequent 38-cm-diameter vessels were coated before and after winding in an attempt to prevent liner leakage. The second vessel failed in the hoop wraps at 34.8 MPa (compared to the 41.4-MPa design pressure). The third vessel leaked excessively at 34.5 MPa; leakage was found to be caused by failure of the

Table 25. Winding pattern for the 38.1-cm-diameter Kevlar/epoxy[a] pressure vessels.

Property	Value
Winding tension, N	26.7
Longitudinal angle, deg (min)	9 (39)
Winding pattern	36-band, closed
Layers (interspersing): hoop	2(3 + 18)
longitudinal	10 (8H + 10L + 18H)
Total winding circuits: hoop	2340
longitudinal	4320
Extra reinforcement at the equator, circuits	56 revolutions per end

[a]Epoxy system XD 7575.02/XD 7818/ERL 4206/Tonox 60-40 (50/50/30/38 parts by weight), gelled for 88 h at 22°C and cured for 5 h at 120°C.

Table 26. Summary of the winding pattern design (wall cross section) for the 10.2-, 20.3-, and 38.1-cm-diameter pressure vessels.

Pattern	Vessel diameter, cm		
	10.2	20.3	38.1
Thickness of butyl rubber liner, cm	0.05	0.05	0.05
Inner hoop wraps, cm wound at deg	0.018 at 90	0.06 at 90	0.19 at 90
Longitudinal wraps, cm wound at deg	0.036 at 12.5	0.13 at 7	0.43 at 9.67
Outer hoop wraps, cm wound at deg	0.035 at 90	0.18 at 90	0.48 at 90

inside liner coating at the edges of the flanges on the aluminum bosses. The fourth vessel burst at 35.1 MPa with failure occurring in the hoop wraps.

Because composite performance of these initial four vessels was low (0.212 MPa·m³/kg), a fifth vessel was wound using 1420 denier fiber instead of the 4560 denier fiber. This vessel burst at 32.4 MPa. A high pressurization rate was used during this burst test because of the leakage problems and this rate may have contributed to the poor performance of this fifth vessel. All subsequent vessels were wound from the 4560 denier fiber. The sixth vessel wound failed at 37.2 MPa. The winding pattern for the 38-cm-diameter vessel design was fixed after this sixth vessel and four additional vessels were wound with this pattern. Table 29 gives the winding pattern details and the burst test results of the last four vessels. The average composite performance of these last four vessels was 0.236 MPa·m³/kg for a vessel volume of 43.5 × 10^3 cm³. The average burst pressure was 36.0 MPa.

The relatively low performance of these vessels is attributed to (1) a thick-wall effect, (2) the winding pattern, and (3) residual stresses. A photograph of a typical vessel failed in the hoop wraps is given in Fig. 39 and the recorded hoop strains of the 15-8 and 15-9 vessels (Table 29) are given in Fig. 40. Axial strain measurements are not given in Fig. 40 because erratic gage behavior resulted in erroneous measurements.

Liner Leakage Problem

The rubber/polymer, multilayered liner used successfully in the 10.2-cm-diameter vessel design failed consistently in the 20.3- and 38-cm-diameter vessels. In both of the larger vessel designs, the quality of the butyl rubber was poor. In the early 20.3-cm-diameter vessels, many liners were pitted in the dome section (Fig. 41). We also found that the butyl rubber was not completely cured. The subsequent vapor deposition of the Parylene C onto the incompletely cured rubber resulted in a cell-like formation (see Fig. 42) with

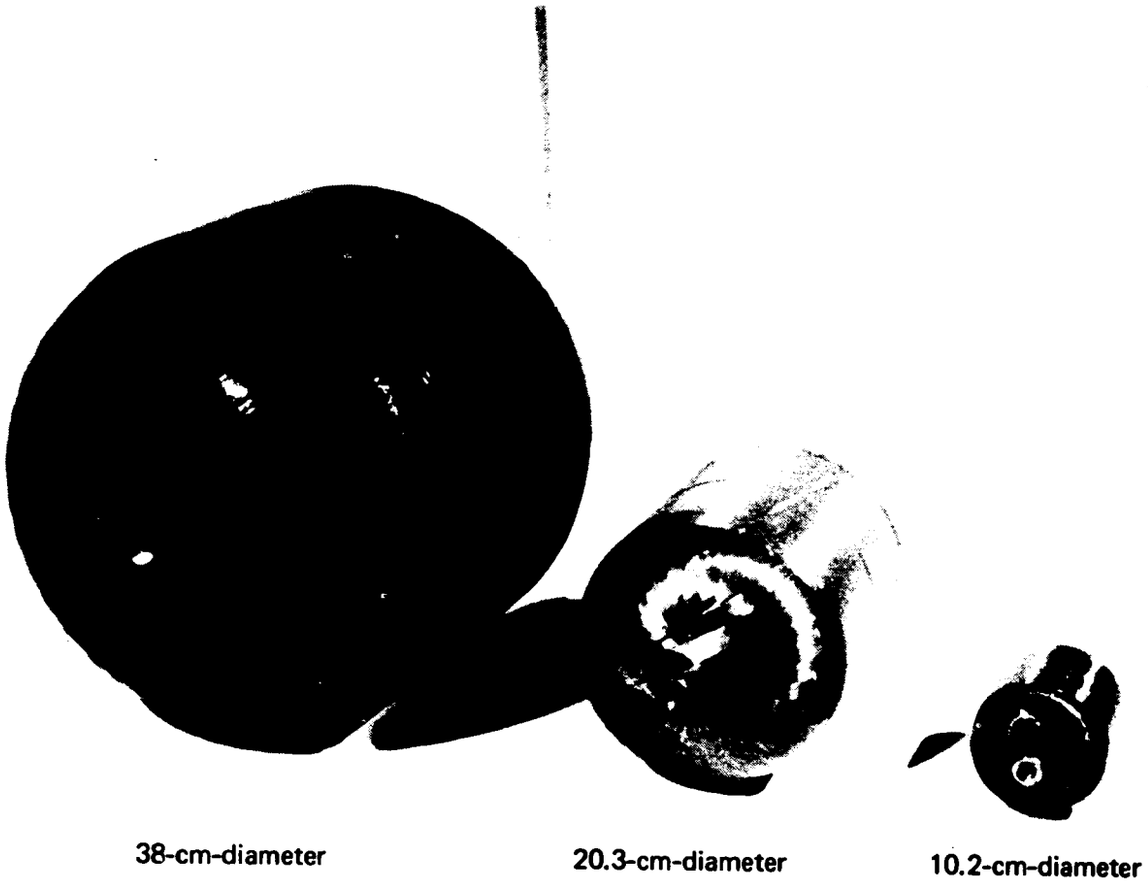

Fig. 36. Photograph of the 10-cm-diameter, 20-cm-diameter, and 38-cm-diameter pressure vessels tested in this study.

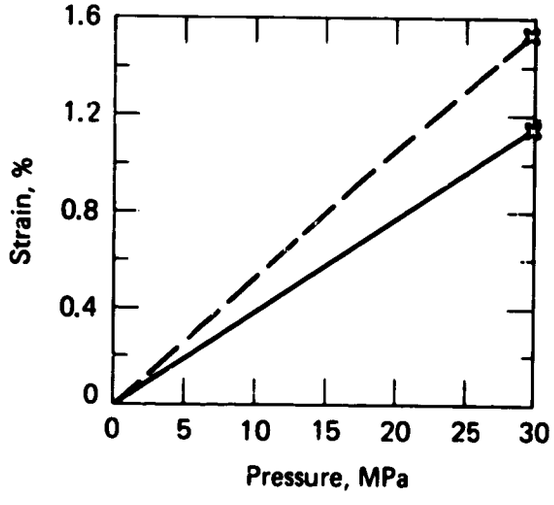

Fig. 37. Recorded axial (dashed curve) and hoop (solid curve) strains for the K-23, 20.3-cm-diameter, rubber-lined Kevlar 49/epoxy pressure vessel.

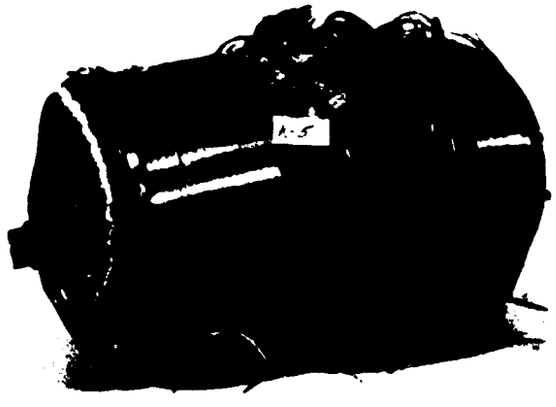

Fig. 38. Photograph of the hoop failure of the K-5, 20.3-cm-diameter pressure vessel.

Table 27. Performance of rubber-lined, 20.3-cm-diameter Kevlar 49/epoxy[a] pressure vessels (0.5-mm-thick liner, 23°C test temperature).

Property	Vessel No.					
	K8	K19	K20	K21	K22	K23
Vessel Data[b]						
Burst pressure, MPa	31.85	28.34	28.96	31.51	29.41	29.17
Failure location[c]	H,F,K	F	F	F	K	F
Fiber performance, MPa·m³/kg	0.445	0.432	0.442	0.445	0.392	0.399
Composite performance, MPa·m³/kg	0.313	0.313	0.321	0.348	0.290	0.289
Composite Data						
Composite mass, kg	0.9620	0.8566	0.8526	0.8556	0.9594	0.9553
Fiber mass, kg	0.6768	0.6196	0.6189	0.6694	0.7101	0.6907
Fiber content, vol%	66.4	68.4	68.5	68.4	70.0	68.4
Winding Data[d]						
Winding tension, N	17.8					
Longitudinal angle, deg	7					
Winding pattern	36-band, closed					
Hoop/longitudinal fiber ratio	1.55					
Layers (interspersing): hoop	16(4 + 12)					
longitudinal	8(none)					
Total winding circuits: hoop	2592					
longitudinal	2592					
Extra reinforcement at the equator, circuits	40 per end					

[a]Epoxy system is XD 7818/T-403 (100/49 parts by weight), gelled for 18 h at 85 C and cured for 3 h at 190 C.

[b]Vessel volume is a constant 9.453×10^{-4} m³.

[c]H = hoop failure, F = fitting failure, K = knuckle failure.

[d]Winding data are the same for all six vessels.

no coating at the boundaries of the cells. We determined that vaporization of dissolved solvents in the rubber was the cause of this problem. The problems with the Saran-lined vessels may have resulted from the fact that we painted the Saran coating on the larger mandrels; apparently, this did not give as good a coating as spray application.

Table 28. Averaged performance of vessels K8, K19, K20, K21, K22, and K23.

Property	Average Value	CV, %
Vessel Data[a]		
Burst pressure, MPa	29.87	5
Failure location	Fitting	—
Fiber performance, MPa·m³/kg	0.426	6
Composite performance, MPa·m³/kg	0.312	7
Composite Data		
Composite mass, kg	0.9069	6
Fiber mass, kg	0.6642	6
Fiber content, vol%	68.4	2

[a]Vessel volume is a constant 9.453×10^{-4} m³.

Four micrographs of wall sections taken from vessels with these liner problems are shown in Fig. 43. The dark centermost zone in Figs. 43a and 43b is the rubber liner of a 20.3-cm-diameter vessel. These two micrographs dramatize the extent of the voids typically found. Figures 43c and 43d illustrate one effect of an inadequately cured rubber liner: in this instance, the rubber migrated into the composite wall of the vessel (10.2-cm-diameter) during composite curing. Post-curing the butyl rubber for 3 h at 121 C still did not solve the problem. Static burst tests were successful but cyclic fatigue testing resulted in rapid failure in the liners.

Early 38-cm-diameter vessels could not be burst because of excessive liner leakage. We tried various coating schemes to prevent this. The rubber liners of the second and third 38-cm-diameter vessels were coated with two layers of Saran separated by a layer of flexible epoxy before winding, and coated inside with urethane rubber after winding. Both vessels still

Table 29. Performance of rubber-lined, 38.1-cm-diameter Kevlar/epoxy pressure vessels (0.102-cm-thick liner, 23°C test temperature).

Property	Vessel No.			
	15-7	15-8	15-9	15-10
Vessel Data[a]				
Volume, m^3	43.525	43.525	43.525	43.525
Burst pressure, MPa	37.5	35.2	36.6	34.5
Failure location[b]	K	K	H	H
Fiber performance, $MPa \cdot m^3/kg$	0.342	0.323	0.335	0.326
Composite performance, $MPa \cdot m^3/kg$	0.247	0.230	0.245	0.233
Composite Data				
Composite mass, kg	6.600	6.675	6.500	6.725
Fiber mass, kg	4.770	4.7492	4.7516	4.609
Fiber content, vol%	68.2	67.2	69.2	64.3

[a]See Table 9 for vessel winding pattern.

[b]H = hoop failure, F = fitting failure, K = knuckle failure.

leaked because of failure of the inside coating at the edges of the flanges of the aluminum bosses.

We also evaluated several coating systems for their ability to patch leaking rubber-liner vessels. All tests were made with 20.3-cm-diameter vessels: Table 30 summarizes these results. The best system, based on successful burst tests and processing ease, was the Mereco 4501 epoxy applied in thicknesses of 0.76 to 1.27 mm.

By modifying the coating technique used for the outside of the rubber mandrel and by choosing a successful filament winding pattern, we were able to manufacture 20.3-cm-diameter, polymer-lined Kevlar/epoxy vessels that held nitrogen gas at about 50% of the vessel burst pressure for 3 mo with a steady state leak rate of less than 0.4% per month. Four vessels then were fabricated in the same way, except that the following coating procedure was used. First, the mandrel surface was cleaned with acetone and allowed to air dry for 2 h. Then, a 0.005-cm-thick layer of XD 7151 Saran latex was applied. Next, two separate coatings of epoxy (XD 7575.02/DER 732/ethanolamine, 80/20/11.9 parts by weight) were applied approximately 4 h

Fig. 39. Photograph of the hoop failure of a 38-cm-diameter, Kevlar 49/epoxy pressure vessel.

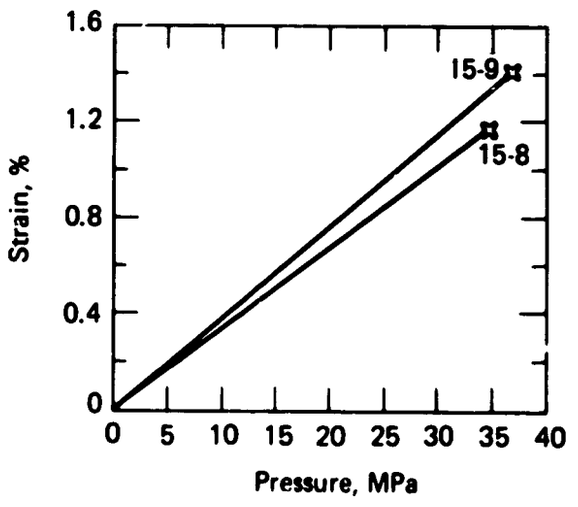

Fig. 40. Recorded hoop strains for the 15-8 and 15-9, 38-cm-diameter, rubber-lined, Kevlar 49/epoxy pressure vessels.

Fig. 41. Photograph of the interior of the K-11, 20.3-cm-diameter pressure vessel showing the pitted Parylene C liner.

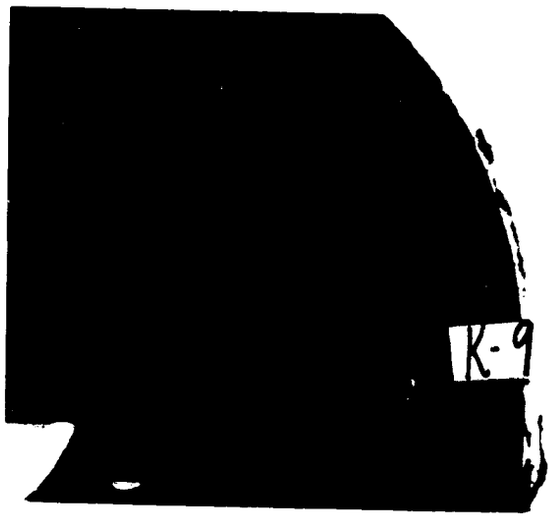

Fig. 42. Photograph of the interior of the K-9, 20.3-cm-diameter pressure vessel showing the cell-like structure of the Parylene C liner.

apart; a total of about 50 g of epoxy was used. Another layer of Saran latex XD 7151, 0.015 cm thick, was applied. Finally, the vessel was painted with the epoxy XD 7818/T-403.

One other change made in the vessel fabrication procedure was that the winding tension for the first two hoop layers and the first longitudinal layers was reduced from 17.8 N (normal tension) to 8.9 N. These changes in coating procedure and winding tension alleviated the problem of coating cracking sufficiently so that the vessels would hold nitrogen gas at 50% of burst pressure. Unfortunately, these vessels all leaked fluids at about 70% of the expected failure pressure when we tried to burst them after the gas permeation test.

On the basis of our results, we speculate that the most likely causes of liner failure in the 20.3-cm-diameter vessel are (1) increase in the pressure in the 20.3-cm-diameter vessel over that in the 10.2-cm-diameter vessel, (2) poor quality of the rubber liner, and (3) cracks in the composite matrix that propagate into the polymer liners.

New Concepts

Several new liner material systems and design concepts were studied in an attempt to solve the problems described above. Specifically, we considered (1) a styrene liner with a 0.20-to-0.28-mm-thick coating of Saran, (2) a styrene liner with a 0.075-to-0.13-mm-thick coating of flexible epoxy, (3) a one-piece, 0.75-mm-thick

Table 30. Various liner coatings tested in an attempt to improve pressure vessel performance (i.e., increase burst pressure, decrease permeability).

Coating	No. of tests	Successful	Thickness
Turco 5145 (solvent coating)	1	No	0.13
50% Dow Corning 92-009 in UM and P (naphtha)	1	No	0.84
Hexcel 7200 (urethane)	2	No	0.51
Butarez CTL II/ ERL 0510/N,N-DMBA (polybutadine rubber)[a,b]	1	Yes	0.76
Mereco 4501 (epoxy)	2	Yes	1.27 1st test 0.76 2nd test

[a]100/10/0.5 parts by weight.
[b]Material more viscous than desirable.

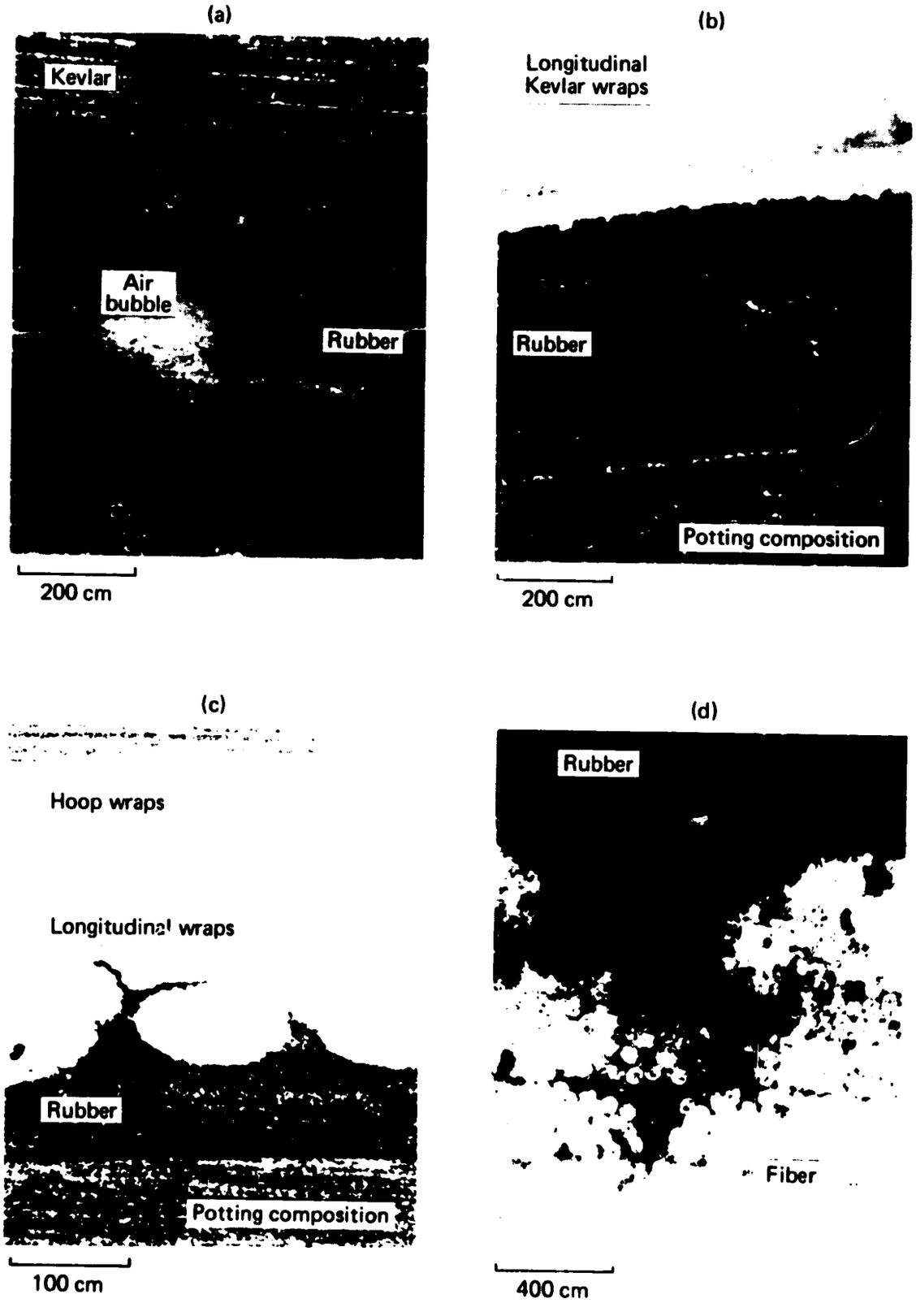

Fig. 43. Photomicrographs of four wall sections illustrating some of the problems with the liners: (a, b) 20.3-cm-diameter vessels with voids, (c, d) 10.2-cm-diameter vessels with rubber migration.

Fig. 44. Photograph of an ABS-lined pressure vessel wound with the double pattern overwind showing the hoop mode of failure (vessel failed at 36.8 MPa).

ABS liner, and (4) a joined two-piece, 0.75-mm-thick ABS liner. Fiber Science Co. was contracted to supply the ABS liners; they were not able to fabricate the one-piece ABS liner so this concept has not been evaluated. All vessels tested with these new liners were 10.2 cm in diameter and were wound as described in the previous study.

The coated styrene liners gave poor performance. Leaks developed in four vessels at pressures below 10.3 MPa. Liner cracks were evident in the tested vessels. The general quality of these liners was poor; they seemed to possess insufficient flexibility for the application. Four additional vessels with coated styrene liners burst during pressurization at pressures below 14 MPa. The failures in these vessels were located in the end or knuckle regions and may have originated near the edge of the boss flange or at nonsymmetrical regions of the liners.

Seven vessels with the two-piece ABS liner were manufactured. The first two vessels used a single winding pattern. One of these vessels was burst at 15 MPa for a performance factor of 0.138 MPa·m³/kg: failure was in the hoop wraps. The second vessel wound with the single pattern leaked. The cause of this leakage was thought to be poor alignment between the liner halves. The last five vessels with the two-piece ABS liner used the double winding pattern in an attempt to improve vessel performance so we could evaluate liner performance at higher pressures. The best performing of these vessels burst in the hoop wraps at 36.8 MPa for a performance factor of 0.23 MPa·m³/kg. The total vessel weight of this vessel was 148 g, of which the liner contributed 30 g and the bosses 31 g. A photograph of a burst ABS-lined vessel is given in Fig. 44.

Of these new liner systems, only the two-piece ABS liner produced a high performance vessel. These liners, however, are heavier than the earlier polymer liners. In addition, we did not perform any permeation or fatigue cycling tests nor did we fabricate any larger vessels with these new liners. Therefore, we cannot advocate their use at this time.

Conclusions

From these studies of Kevlar fiber/epoxy pressure vessels with various polymer liners, we draw the following conclusions:

- The 10.2-cm-diameter, cylindrical, Kevlar/epoxy pressure vessels lined with combinations of chlorobutyl rubber, Saran, and Parylene C have a nitrogen gas pressure loss rate of less than 1% per month when pressurized to 65% (about 11.7 MPa) of their expected burst pressure at 21°C.
- These same 10.2-cm-diameter pressure vessels have a composite performance factor of approximately 0.370 MPa·m³/kg or a performance factor based on total vessel weight (excepting the metal fittings) of approximately 0.200 MPa·m³/kg.
- Comparison of the calculated pressure loss rates with the experimental values indicates that the Parylene C coating may be just as effective as Saran for reducing the nitrogen gas loss.
- The fatigue life of the Kevlar/epoxy pressure vessel depends on both the number of stress cycles and the time at peak load during each stress cycle.
- The fatigue life of the Kevlar/epoxy pressure vessels cycled to 91% of the mean burst pressure can range fifty- to sixty-fold. The burst pressure of 25 vessels randomly selected from a population of 150 identically manufactured vessels has a CV of 4.5% when all vessels fail in the same location (i.e., hoop wraps).
- The fatigue life of the Kevlar/epoxy vessels cycled sinusoidally between 4 and 91% of the mean burst pressure at a test rate of 1 Hz is about six times longer than the life for vessels cycled with a rectangular pressure cycle at a test rate of 0.33 Hz.
- Scaling up of the 10.2-cm-diameter, polymer-lined Kevlar/epoxy pressure vessel was not successful because of a persistent problem with liner leakage.
- Of the new liner concepts tested, the two-piece ABS liner with a double pattern overwind was a limited success. This liner gave good performance without leakage during pressurization. However the ABS liner was tested only in a 10.2-cm-diameter vessel and no gas permeation or fatigue cycling tests were performed.
- Liners of pure Parylene C leak. Styrene liners were of poor quality and were not flexible enough, resulting in leakage during pressurization.
- At the present time, there is no proven polymer liner system that offers the required low permeability and high flexibility.
- Nonleaking polymer liners are three times as thick as successful titanium-liners. Hence, there are no significant weight savings in using polymeric materials. The lack of consistency of the polymer liners as leak-free systems also indicates that with present technology, they are unreliable.
- In addition, polymer liners are of limited use because they only prevent the permeation of nitrogen gas. They do not successfully meet the cyclic lifetime requirement. However, recent fatigue results with thin titanium liners indicate that sufficient fatigue life can be obtained.
- Because the present polymer liners must be thicker than metal liners to be impermeable to nitrogen gas, any possible weight saving is cancelled. Also,

polymer liners do not meet the fatigue lifetime requirements. Thus the major reasons for using polymer liners in composite pressure vessels are no longer valid.

References

19. M. A. Hamstad, T. T. Chiao, and E. S. Jessop, "Polymer-Lined Filament Wound Pressure Vessels for Nitrogen Containment," presented at *AIME Spring Meeting, Failure Modes in Composites II*, May 21-22, 1974, Pittsburgh, PA.

20. T. T. Chiao, M. A. Hamstad, and M. A. Marcon, *Organic Fiber/Epoxy Pressure Vessels*, Lawrence Livermore Laboratory, Preprint UCRL-75098 (1973).

21. T. T. Chiao and M. A. Marcon, "Filament Wound Vessel from an Organic Fiber/Epoxy System," in *Proc. S.P.I. Reinforced Plastics/Composites Division*, Section 9b (1973).

22. M. A. Hamstad, T. T. Chiao, and R. G. Patterson, "Fatigue Life of Organic Fiber/Epoxy Pressure Vessels," in *Proc 7th Natl. SAMPE Tech. Conf.*, October 14-16, 1975, Albuquerque, NM.

23. M. A. Hamstad, R. H. Toland, and T. T. Chiao, *Lightweight Composite Pressure Vessels*, Lawrence Livermore Laboratory, Rept. UCID-17176 (1976).

24. M. A. Hamstad, E. S. Jessop, and R. H. Toland, *Advanced Technology for Minimum Weight Pressure Vessel Systems*, Lawrence Livermore Laboratory, Rept. UCID-17399 (1977).

PLL